THE UNIVERSITY OF ALBERTA

LINEAR ANALYSIS OF TWO INSECT MECHANORECEPTORS

by

© Arun V. Holden

A THESIS

SUBMITTED TO THE FACULTY OF GRADUATE STUDIES

IN PARTIAL FULFILMENT OF THE REQUIREMENTS FOR THE DEGREE

OF DOCTOR OF PHILOSOPHY

DEPARTMENT OF PHYSIOLOGY

EDMONTON, ALBERTA

FALL, 1971

UNIVERSITY OF ALBERTA

FACULTY OF GRADUATE STUDIES

The undersigned certify that they have read , and recommend to the Faculty of Graduate Studies for acceptance , a thesis entitled Linear Analysis of Two Insect Mechanoreceptors submitted by Arun V. Holden in partial fulfilment of the requirements for the degree of Doctor of Philosophy .

R B Stein

Supervisor

H G Pearson

R Smith

R B Stein

R. E. Poole

Jack D. Cowan

External examiner

Date 7th June 1971

ABSTRACT .

Spectral analysis provides powerful techniques for the approximate linear analysis of the input-output relations of a system . When a system is subjected to a stochastic , band-limited driving function estimates of the frequency response function , the coherence function and the information transmission rate may be obtained from consistent spectral and cross- spectral estimates .

One problem in applying spectral analysis to a primary sensory neurone is that the response of the neurone is a spike train . A method of obtaining regular , alias-free samples of a spike train with an arbitrary sampling rate has been developed . Using a package for consistent spectral and cross-spectral estimation the frequency response functions , coherence functions and information transmission rates of two insect mechanoreceptors have been estimated . Both these receptors have frequency response functions indicating a high-pass filter characteristic , and a coherence function which is never greater than 0.5 . The low coherence function indicates that the response of the receptor is noisy and nonlinear , and so the frequency response function is not an accurate characterization of the input-output characteristics of the receptors .

TABLE OF CONTENTS .

LIST OF FIGURES .

CHAPTER 1 .

INTRODUCTION .

Following Pringle and Wilson's (1952) use of linear systems theory to characterize the input-output relations of an insect mechanoreceptor linear systems theory has been used to investigate the signal transfer characteristics of a large number of single neurones . It has been applied to receptors (Chapman and Smith, 1963 ; Borsellino, Poppele and Terzuolo, 1965 ; Brown and Stein, 1966 ; Pinter, 1966 ; Houk and Simon, 1967 ; Dodge, Knight and Toyoda, 1968 ; Matthews and Stein, 1969a; Poppele and Bowman, 1970 ; Knight, Toyoda and Dodge, 1970 ; Pearson and Holden, 1970 ; Holden and French, 1971a , 1971b) , higher order sensory neurones (Spekreijse, 1969 ; Maffei, Cervetto and Fiorentini, 1970 ; Melville Jones and Milsum, 1970) , neuro-muscular effectors (Partridge, 1965 ; McKean et al. , 1970) , and synapses (Hagiwara and Morita, 1962 ; Watanabe, 1968) . Some of these , and other examples , are reviewed in the Neurosciences Research Program Bulletin on 'Neural Coding' (Perkel and Bullock, 1968) and the Brainerd conference on 'Systems Analysis in Neuro-physiology' (Terzuolo, 1969) . Linear systems theory provides a powerful body of techniques for investigating the input-output relations of linear systems , and can also be used as a general approach to the approximate analysis of nonlinear systems .

In spite of its widespread application in the study of single

units in the nervous system there are problems in treating a neuronal element as a system with a clearly defined input function x(t) , or set of input functions , and a clearly defined output y(t) . For a primary sensory neurone , the input is a continuous time varying function which may also vary spatially , and the output may be a continuous function , as in photo-receptors (Arden, 1969) or a crab mechanoreceptor (Bush and Roberts, 1968) , but is generally a spike train . For a central neurone , the input may be taken as a large number of spike trains , and the output as a single spike train . For a neuro-muscular effector , the input is a spike train , or number of spike trains , and the output is a continuous function (say tension) . Thus in most cases one or more of the signals is a spike train . Although a recorded spike train is a continuous band-limited signal , since the duration of an action potential is short compared to the mean inter-spike interval , and action potentials are generally all-or none , it is usual to treat a spike train as a series of identical events . An exception to this is given in Gestri, Maffei and Petracchi (1967) and Barbi and Petracchi (1971) .

If all action potentials in a spike train are taken as equivalent events there are two ways in which a spike train may be treated :

i). a continuous function may be generated from the spike train (Terzuolo, 1970) . This may be the averaged interval between spikes , the rate of spikes averaged over some time or number of spikes , or an estimate of the probability density of spikes relative to some time marker (the cycle or post-stimulus time histogram). Alternatively , unaveraged , discontinuous functions may be generated .

ii). the spike train can be considered as a realization of a stochastic point process (Moore, Perkel and Segundo, 1966 ; Stein, 1970) or as a series of unit impulses or Dirac delta functions (French and Holden, 1971a ; Knox, 1969)

When a suitable form of describing the spike train has been chosen linear systems theory can be used to derive a relationship between the input signal and the output signal . Such an approach is purely descriptive - the neuronal element is treated as a 'black box' and a mathematical model is formulated which attempts to describe the input-output relations of the black box . However , such a quantitative description is of value in its own right , and may be used as a basis for either dissecting the black box into possible components (see , for example , Terzuolo et al. , 1968) or for building models of simple neuronal networks .

A variety of methods , both in the time domain and in the frequency domain , are available for obtaining a quantitative description of the input-output relations of a system . These methods are reviewed in Chapter 2 and their implementation discussed in Chapter 3 . In later chapters some of these methods are applied to two sensory receptors , the tactile spine of the cockroach and the chordotonal organ of the locust .

CHAPTER 2 .

LINEAR SYSTEMS THEORY .

2.1. Definition of a linear system .

A linear transformation from a vector space Z_1 to a vector space Z_2 is a function A which provides a one-to-one association with each vector z in Z_1 with a vector A(z) in Z_2 such that:

$$A(z_1 + z_2) = A(z_1) + A(z_2) \qquad 2.1$$

and

$$A(\alpha z) = \alpha A(z)$$

for all vectors z in Z_1 and all scalars α . If the vector space Z_1 contains all possible input functions z to a system and the vector space Z_2 contains all possible responses of the system then the system is linear if and only if equation 2.1 is valid for all input functions z and all responses A(z) . This is a statement of the principle of superposition . If the principle of superposition holds for only some of the possible inputs , and not for other inputs , then the system is not linear .

2.2. Application to linear , noise-free systems .

For a linear noise-free system with a single input or driving function x(t) and a single output or response y(t) the output is related to the input by the convolution integral :

$$y(t) = \int_0^t x(\tau)\, g(t,\tau)\, d\tau \qquad 2.2$$

and if the system is also time invariant a function g(t) exists such that

$$y(t) = \int_0^t x(\tau)\, g(t-\tau)\, d\tau \qquad 2.3$$

where g(t) is the weighting function of the system .

Treatment of equation 2.3 is greatly simplified if it is examined in the s domain , where s is a complex variable . This may be achieved by use of the Laplace Tranform (Smith, 1966) . The Laplace Transform is a linear transform and is defined by :

$$\begin{aligned} \text{L.T. } \{y(t)\} &= Y(s) \\ &= \int_0^\infty y\, e^{-st} dt \end{aligned} \qquad 2.4$$

and its inverse is given by

$$\text{L.T.}^{-1} \{Y(s)\} = \frac{1}{2\pi} \int_{c-j\infty}^{c+j\infty} Y(s)\, e^{ts} ds \qquad 2.5$$

where c is a constant which must be defined to ensure convergence in this contour integration . Thus y(t) and Y(s) form a Laplace Transform pair

$$y(t) \leftrightarrow Y(s)$$

In practice it is generally not necessary to evaluate the forward

and inverse transforms as they are available in tables for most commonly encountered functions .

The most useful properties of the Laplace Transform are:

a) Linearity

$$k\,y(t) \quad \leftrightarrow \quad k\,Y(s)$$

$$y(t) + f(t) \quad \leftrightarrow \quad Y(s) + F(s)$$

b) Time translation

$$y(t-\tau) \quad \leftrightarrow \quad e^{-\tau s}Y(s)$$

c) Real convolution

$$\int_0^t y(t-\tau)\, f(\tau) \quad \leftrightarrow \quad Y(s)F(s)$$

Application of the convolution property to the Laplace Transform of equation 2.3 yields

$$Y(s) = G(s)\,X(s) \qquad 2.6$$

When the input function x(t) is a unit impulse or Dirac delta function $\delta(t)$ such that

$$\int_{-\infty}^{\infty} \delta(t)\,dt = 1$$

$$\delta(t) = 0\,,\ t \neq 0 \qquad 2.7$$

the Laplace Transform of x(t) is unity and so equation 2.6 now gives

$$Y(s) = G(s)$$

Thus the Laplace Transform of the response to a unit impulse is the Laplace Transform of the weighting function g(t) of the system .This is the transfer function , G(s) , of the system which is only defined for a linear , time invariant and noise-free system . The transfer function completely characterizes the input-output relations of the system .

An alternative representation of the transfer function is the frequency response function G(f) given by

$$G(f) = \int_0^\infty g(t)\, e^{-j2\pi ft} dt \qquad 2.8$$

where in place of the Laplace Transform we are using the one-sided Fourier Transform .

The frequency response function is complex and in engineering contexts its magnitude is generally plotted as the dimensionless ratio gain in dB. . However , although this convention is often used in neurophysiology (e.g. : Poppele and Bowman, 1970) it is inappropriate when the input and output signals do not have the same dimensions .

When the input x(t) to the system is a realization of a stationary stochastic process one can define the autocovariance function $\rho_{xx}(\tau)$ of x(t) as (Jenkins and Watts, 1968 ; Lee, 1967)

$$\rho_{xx}(\tau) = \lim_{T\to\infty} \frac{1}{2T} \int_{-T}^{T} x(t)\, x(t+\tau)\, dt \qquad 2.9$$

and the autocovariance function $\rho_{yy}(\tau)$ of the response $y(t)$ as

$$\rho_{yy}(\tau) = \lim_{T\to\infty} \frac{1}{2T} \int_{-T}^{T} y(t)\, y(t+\tau)\, dt$$

and the forward cross-covariance $\rho_{xy}(\tau)$ from the input to the output

$$\rho_{xy}(\tau) = \lim_{T\to\infty} \frac{1}{2T} \int_{-T}^{T} x(t)\, y(t+\tau)\, dt \qquad 2.10$$

These covariance functions are the mathematical expectation of the product of the values which the stationary random processes assume at instants separated by τ. i.e. for the autocovariance function of $x(t)$ where $x(t)$ is a realization of an ergodic process.

$$\rho_{xx}(\tau) = E\{ x(t)\, x(t+\tau) \}$$

They are related to the corresponding correlation functions $\gamma_{xx}(\tau)$, $\gamma_{yy}(\tau)$, and $\gamma_{xy}(\tau)$ where σ is the standard deviation by

$$\begin{aligned} \gamma_{xx}(\tau) &= \sigma_x^2\, \rho_{xx}(\tau) \\ \gamma_{yy}(\tau) &= \sigma_y^2\, \rho_{yy}(\tau) \\ \gamma_{xy}(\tau) &= \sigma_x \sigma_y\, \rho_{xy}(\tau) \end{aligned} \qquad 2.11$$

The autocovariances and autocorrelation functions are even functions of τ, the cross-covariance and cross-correlation are generally

odd functions of τ.

From the Wiener-Khinchine relation (Lee, 1967 ; Thomas, 1969) one can obtain the power spectra of the input and the output and the cross-power spectrum from the Fourier Transforms of the corresponding input , output and cross-covariance functions .

The Fourier Transform F(f) of a function f(t) is defined by :

$$F(f) = \int_{-\infty}^{\infty} f(t)\, e^{-j2\pi ft}\, dt \qquad 2.12$$

and the inverse transform by

$$f(t) = \frac{1}{2\pi} \int_{-\infty}^{\infty} F(f)\, e^{j2\pi ft}\, dt \qquad 2.13$$

where $j = \sqrt{-1}$.

Thus the input power spectrum $S_{xx}(f)$, the output power spectrum $S_{yy}(f)$ and the cross-power spectrum $S_{xy}(f)$ are given by:

$$S_{xx}(f) = \int_{-\infty}^{\infty} \rho_{xx}(\tau)\, e^{-j2\pi f\tau}\, d\tau$$

$$S_{yy}(f) = \int_{-\infty}^{\infty} \rho_{yy}(\tau)\, e^{-j2\pi f\tau}\, d\tau \qquad 2.14$$

$$S_{xy}(f) = \int_{-\infty}^{\infty} \rho_{xy}(\tau)\, e^{-j2\pi f\tau}\, d\tau$$

Note that $S_{xx}(f)$ and $S_{yy}(f)$ are real , even functions while $S_{xy}(f)$ is complex and odd . $S_{xy}(f)$ is often considered in terms of its real part , the real- valued even co-spectrum $C_{xy}(f)$ and its

imaginary part , the real-valued odd quad-spectrum $Q_{xy}(f)$ where

$$S_{xy}(f) = C_{xy}(f) - jQ_{xy}(f) \qquad 2.15$$

or alternatively

$$C_{xy}(f) = S_{xy}(f) + S_{yx}(f)$$

$$Q_{xy}(f) = j[\, S_{xy}(f) - S_{yx}(f) \,]$$

where $S_{yx}(f)$ is the backward cross-spectrum .

These spectra are two-sided , that is they are defined for negative as well as positive frequencies . Although two-sided spectra simplify the analysis , in most applications negative frequencies do not have a physical interpretation , and so from the two-sided spectra one can obtain one-sided spectra defined only for positive frequencies by folding the two-sided spectrum over the zero frequency axis so that the one sided spectrum is given by

$$R_{xx}(f) = \begin{cases} 2S_{xx}(f) & 0 < f < \infty \\ 0 & f < 0 \end{cases} \qquad 2.16$$

Since the cross-spectrum is odd , to obtain its one-sided spectrum the two-sided spectrum has to be folded over both axes .

From either the one or two-sided spectra one can obtain the frequency response function from the following relations :

$$G(f) = \frac{S_{xy}(f)}{S_{xx}(f)} \qquad 2.17$$

or

$$G(f) = \frac{S_{yy}(f)}{S_{yx}(f)} \qquad 2.18$$

and

$$S_{yy}(f) = | G(f) |^2 \; S_{xx}(f) \qquad 2.19$$

Note that the frequency response function G(f) can be interpreted as a complex linear regression coefficient for obtaining y(t) from x(t) (Benignus, 1969a).

2.3. Application to linear systems with intrinsic noise .

If the response y(t) of the system is contaminated by additive intrinsic noise then equation 2.3 does not hold and a transfer function may not be defined . The response will be given by

$$y(t) = \int_0^t x(\tau) \; h(t -\tau) \, d\tau + n(t) \qquad 2.20$$

where n(t) is that part of the output due to the intrinsic noise and h(t) is the weighting function of the linear system .

In this case a describing function may be defined whose frequency response function H(f) is given by

$$H(f) = \int_0^\infty h(t) \, e^{-j2\pi ft} \, dt \qquad 2.21$$

Note that the describing function does not completely characterize the input-output relations of the system , it provides the best (in

the sense of minimum mean squared deviations) linear model for the system .

If the input signal to the system is a realization of a broad-band stochastic process one can define the coefficient of coherence (Tick, 1963 ; Enochson and Goodman, 1965 ; Bendat and Piersol, 1966 ; Benignus, 1969b) by

$$\gamma^2(f) = \begin{cases} \dfrac{|\, S_{xy}(f) \,|^2}{S_{xx}(f).\, S_{yy}(f)}, & S_{xx}(f).S_{yy}(f) > 0 \\ 0 \quad , & S_{xx}(f).S_{yy}(f) = 0 \end{cases} \qquad 2.22$$

Alternative definitions of coherence have been proposed . Wiener (1930) defined a coefficient of coherency as

$$\gamma(f) = \frac{S_{xy}(f)}{[\, S_{xx}(f).S_{yy}(f)]^{1/2}}$$

and this is a complex function which is not invariant when the x(t) and y(t) are subjected to linear transformations . Foster and Guinzy (1967) and Hinich and Clay (1968) define the coefficient of coherence $\gamma(f)$ as the positive square root of the right hand side of equation 2.22 , which although it is a real number and is invariant when the x(t) and y(t) are subjected to linear transformations has been described (Tukey, 1967) as'an unlikely quantity'.

The definition of equation 2.22 has been used because of its analogy with the coefficient of determination (the square of the correlation coefficient) between two random variables . The coherence

function is a normalized measure of the linearity of the relation between $x(t)$ and $y(t)$ and since the spectral matrix

$$S(f) = \begin{bmatrix} S_{xx}(f) & S_{yx}(f) \\ S_{xy}(f) & S_{yy}(f) \end{bmatrix}$$

is non-negative definite (Koopmans, 1964)

$$|S_{xy}(f)|^2 \leq S_{xx}(f) . S_{yy}(f)$$

and so

$$0 \leq \gamma^2(f) \leq 1 \qquad 2.23$$

$\gamma^2(f)$ represents that proportion of $S_{yy}(f)$ which may be accounted for by linear regression onto $S_{xx}(f)$, and $(1 - \gamma^2(f))$ represents that proportion which cannot be accounted for by linear regression . In this case this is the proportion of $S_{yy}(f)$ due to $S_{nn}(f)$, where $S_{nn}(f)$ is the power spectrum of the noise $n(t)$.

From equation 2.20 it can be shown that (Amos and Koopmans, 1963)

$$\gamma^2(f) = \frac{1}{1 + \dfrac{S_{nn}(f)}{S_{xx}(f)\ |H(f)|^2}} \qquad 2.24$$

From this expression Stein and French (1970) have obtained a relationship between the coherence function and the information transmission rate of the system . Shannon (1948) derives the channel capacity in bits/second of a noisy channel for continuous signals as

$$C = \int_0^W \log_2 \left(1 + \frac{S_{ss}(f)}{S_{nn}(f)} \right) df \qquad 2.25$$

where $S_{ss}(f)$ is the signal spectrum and $S_{nn}(f)$ the noise spectrum , both of which are band-limited to W . From equation 2.24 and 2.25 the rate of information transmission is approximately I bits/second where

$$I \sim - \int_0^W \log_2 \left(1 - \gamma^2(f) \right) df \qquad 2.26$$

An important property of the coherence function is its invariance under linear operations (Koopmans, 1964) . This means that the physical systems used to measure x(t) and y(t) will not influence the value of the coherence function if the measuring systems are linear.

2.4. Application to nonlinear systems with intrinsic noise .

For a zero memory nonlinearity, that is , one whose output at a given time depends only on the input at the same time , Booton (1952) has shown that for a given input function x(t) there is an equivalent quasi-linear element $K_{eq}(f)$ such that the mean squared difference between the response of the nonlinear element and the response of the quasi-linear element is minimized . Thus analagous to equation 2.20 the response of the nonlinear system is related to the input by

$$y(t) = \int_0^\infty x(t)\, k(t - \tau)\, d\tau + N(t) \qquad 2.27$$

where N(t) is due to the nonlinear terms in the response and to any intrinsic noise .

In this case the describing function K(f) may be defined by equations similar to those of section 2.3 , and the coherence function provides a measure of that part of $S_{yy}(f)$ which is linearly dependent on $S_{xx}(f)$ and $(1 - \gamma^2(f))$ provides a measure of that part of $S_{yy}(f)$ which is due either to nonlinear transformation of $S_{xx}(f)$ or to intrinsic noise .

Equation 2.27 is not a general representation of the response of a nonlinearity.. A more general representation of the response of a nonlinear system is :

$$y(t) = \Phi[\int_0^\infty x(t)\ k(t - \tau)\ d\tau + n(t)]$$

where n(t) is a noise term and $\Phi[\cdot]$ is a nonlinear operator. However, this general approach is not very tractable.

CHAPTER 3.

ANALYTICAL TECHNIQUES.

3.1. Hardware.

All experimental data (analog signals and spike trains) was recorded on a four channel FM tape recorder (Thermionic T 3000) for subsequent analysis on a Digital Equipment Corporation LAB-8 computer. The computer configuration used consisted of:

1). an 8/I central processor with 4 K of core memory and an extended arithmetic element KE 8/I

2). an AX08 Laboratory Peripheral with four pulse inputs, a four channel multiplexed analog-to-digital convertor (ADC), a crystal and an RC clock and a storage display oscilloscope

3). a DF 32 magnetic disc unit and controller, with 32 K twelve bit words of storage

4). a digital input buffer capable of accepting ten pulse train inputs simultaneously.

The principal flow paths of the data processing system are given in Figure 3.1. Since the pulse outputs (0 → +5V) from the pulse height analyzer units (Stein, 1968a) are incompatible with the pulse input sockets of the AX08, which require 0 → -3V , the digital input buffer was used for all spike train inputs via the pulse height analyzer. A further advantage of using the digital input buffer is that it operates in interupt mode , and so the processor can perform data processing operations while accepting data. The ADC accepts voltages in the range

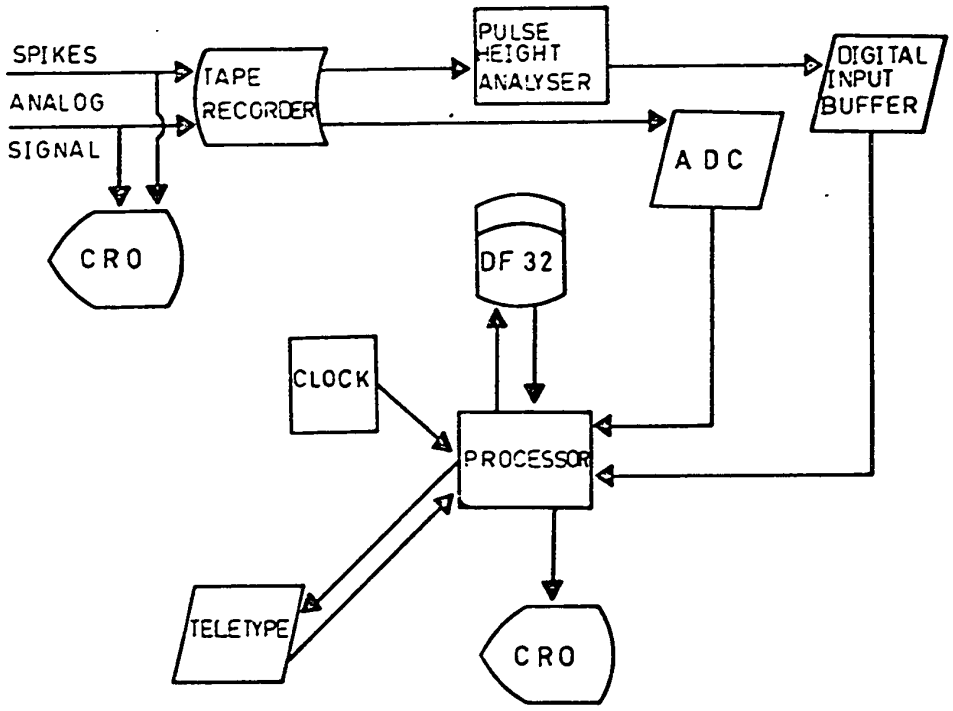

Figure 3.1 . Principal information flow-paths of data processing system .

$\pm$ 1.024 V full scale, , and operates by successive approximation to nine bits . Since the output from the Thermionic tape recorder is limited to $\pm$ 1 V the analog signals could be fed directly to the ADC .

Data output from the system was either via the storage oscilloscope by photography or via the teletype .

3.2. Time domain processing of spike trains.

All time domain processing of spike trains was accomplished using the PULSE and FNEW-PULSE programs (French, 1970) . PULSE is a general purpose histogramming program which accepts two pulse trains . It constructs a histogram with a variable delay (0 to 0.4095 seconds) , a variable number N of bins (1 to 128) of bin width B.100 μseconds , a variable number of events/sweep and a variable number of sweeps. These terms are defined in Figure 3.2 .

FNEW-PULSE provides a means of accessing the stored histogram by the higher level interpretive language FOCAL . This permits fitting the histogram by an appropriate curve.

A cycle histogram may be built up when the spike train is the response to a periodic driving function . Such a histogram results when the trigger pulse is synchronized to the driving function and the product N.B is set to the period of the driving function , and the number of events/sweep is large. A cycle histogram is an estimate of the probability density of spikes as a function of the phase of the periodic driving function .

An interspike interval histogram may be built up when the number of events/sweep is one and the spike train is serving as the trigger pulse . If the number of events/sweep is large an auto-correlogram is formed .

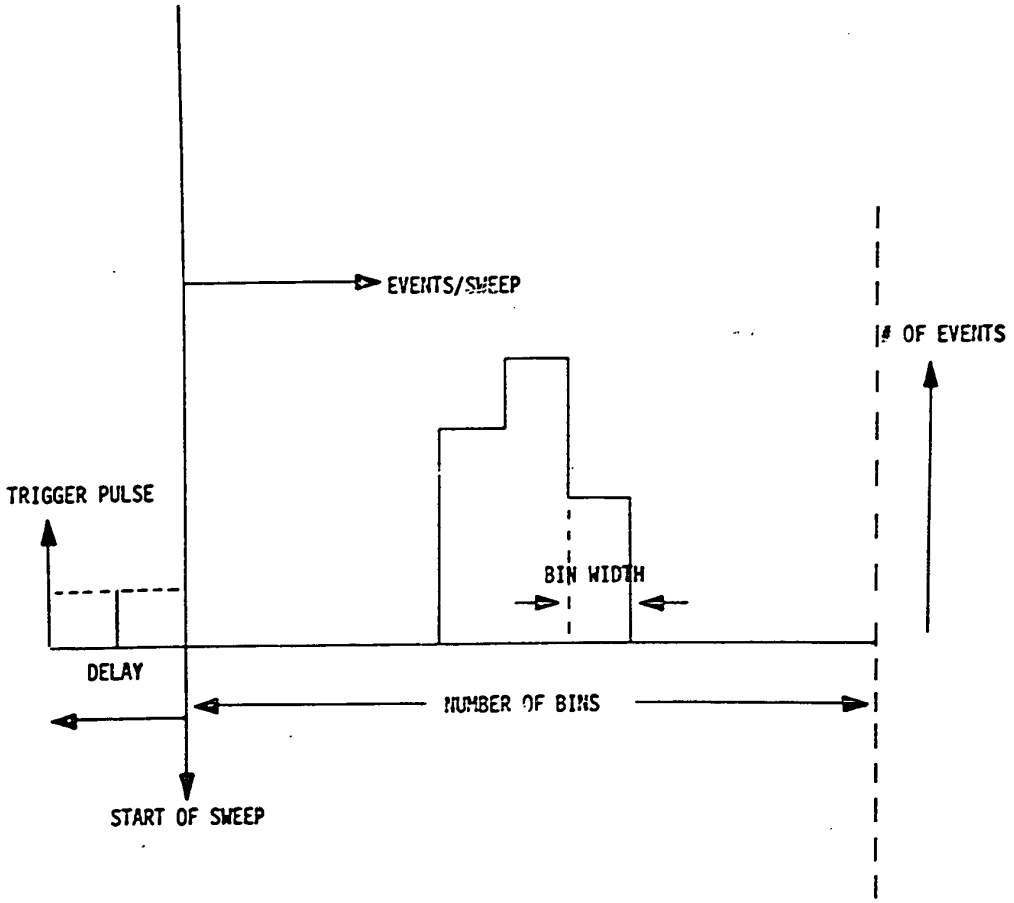

Figure 3.2 . Diagram of example histogram defining the parameters of section 3.2 .

3.3. Methods of spectral estimation.

The power spectra defined by equations 2.14. are obtained from time functions f(t) where $-\infty < t < +\infty$. In practice only a finite realization

$$f_T(t) = \begin{cases} f(t) & 0 \leqslant t \leqslant T \\ 0 & T < 0,\ t > T \end{cases} \qquad 3.1$$

is available and so in place of the power spectra one can define an estimate of the power spectrum , the sample spectrum (Jenkins and Watts, 1968) . Thus in place of equation 2.14a the sample spectrum is given by :

$$\hat{S}_{xx}(f) = \int_{-T}^{T} \hat{\rho}_{xx}(\tau)\, e^{-j2\pi f\tau}\, d\tau \qquad 3.2$$

where $\hat{\rho}_{xx}(\tau)$ is a sample auto-covariance function given by:

$$\hat{\rho}_{xx}(\tau) = \frac{1}{2T} \int_{-T}^{T} x(t)\, x(t+\tau)\, dt \qquad 3.3$$

An alternative definition of $S_{xx}(f)$ may be given by:

$$\hat{S}_{xx}(f) = \frac{1}{T} \int_0^T x_T(t)\, e^{-j2\pi ft} dt \int_0^T x_T(t')\, e^{j2\pi ft'} dt'$$

$$= \frac{1}{T}\, X_T(f) \cdot X_T^*(f)$$

$$= \frac{1}{T}\, |X_T(f)|^2 \qquad 3.4$$

where $X_T(f)$ is the Fourier Transform of $x_T(t)$ and $X_T^*(f)$ is its complex conjugate.

There are a variety of methods available for obtaining the sample spectrum $\hat{S}_{xx}(f)$ and these methods may be considered in three groups :

1) Blackman-Tukey methods

2) Direct methods

3) Auto-regressive methods.

An alternative classification of available methods is given in Parzen (1968).

The Blackman-Tukey , or indirect , methods follow from equations 3.1 and 3.2 (Blackman and Tukey, 1958 ; Jenkins and Watts, 1968) . In order to obtain an estimate of the spectrum from $x_T(t)$, the auto-covariance function $\rho(\tau)$ is estimated by :

$$\hat{\rho}_{xx}(\tau) = \begin{cases} \frac{1}{T}\int_0^{T-|\tau|} x_T(\tau)\, x_T(t+|\tau|)dt, & 0 < |\tau| < T \\ 0 & |\tau| > T \end{cases} \qquad 3.5$$

This estimate of the auto-covariance function is only considered up to a a lag $\tau = W$ where $W << T$. Thus the auto-covariance function estimate has been multiplied by a function $w_r(\tau)$ given by :

$$w_r(\tau) = \begin{cases} 1 & |\tau| \leq W << T \\ 0 & |\tau| > W \end{cases} \qquad 3.6$$

Alternatively , the auto-covariance estimate has been viewed through a rectangular lag window of width 2W. Since multiplication in the time domain is equivalent to convolution in the frequency domain this means that the spectral estimate $\hat{S}_{xx}(f)$ has been convolved with $W_r(f)$ where $W_r(f)$ is the Fourier Transform of $w_r(\tau)$ given by :

$$W_r(f) = 2W\left\{\frac{\sin 2\pi fW}{2\pi fW}\right\} \qquad -\infty \leq f \leq \infty \qquad 3.7$$

and so the spectral estimate is given from equation 3.2 as :

$$\tilde{\hat{S}}_{xx}(f) = \int_{-\infty}^{\infty} W_r(g)\, \hat{S}_{xx}(f - g)\, dg \qquad 3.8$$

$\tilde{\hat{S}}_{xx}(f)$ is a smoothed spectral estimate since the effect of the convolution of $\hat{S}_{xx}(f)$ with $W_r(f)$ is to spread the component at a frequency f over $(\sin 2\pi fW)/2\pi fW$ for $-\infty < f < \infty$ .This spreading of the component at f to other frequencies is called leakage from the frequency f. The decay of the leakage away from the frequency f is shown in Figure 3.3 . $\tilde{\hat{S}}_{xx}(f)$ is an unbiased estimator of $S_{xx}(f)$ if $S_{xx}(f)$ is a slowly varying function of f. However, if the spectrum $S_{xx}(f)$ contains large fluctuations there will be considerable leakage and hence $\tilde{\hat{S}}_{xx}(f)$ will be a biased estimator . This bias may be reduced by quadratic modification , in which lag windows other than $w_r(\tau)$ are used . A desirable property of these lag windows is that their spectral equivalents should have lower and faster decaying side lobes than $W_r(f)$. One result of using the rectangular lag window is that the variance of $\tilde{\hat{S}}_{xx}(f)$ is 2W/T that of $\hat{S}_{xx}(f)$; since $W << T$ this reduction in variance is considerable , and since 2W/T tends to zero as T tends to infinity $\tilde{\hat{S}}_{xx}(f)$ is a consistent estimator of $S_{xx}(f)$.

The Blackman-Tukey approach has been extended to the estimation of cross-spectra (Jenkins and Watts, 1968) and has been extensively modified , notably in the choice of the optimal lag window (Akaike, 1962) . Discussion of the statistical properties of the application of the Blackman-Tukey approach to estimation of open-loop frequency response functions have been given (Jenkins, 1963 ; Akaike and Yamanouchi, 1962 ; Akaike, 1964) .

The direct method of spectral estimation follows from equation 3.4 ,

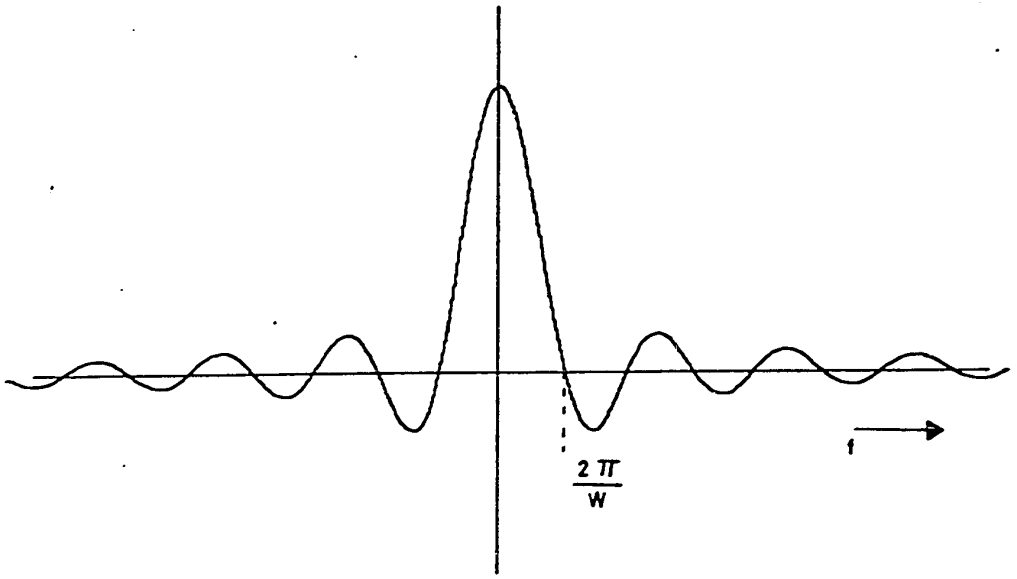

Figure 3.3 . Fourier Transform of rectangular lag window .

and it has only become computationally efficient since the rediscovery of the Fast Fourier Transform algorithm by Cooley and Tukey (1965), which provides an economical method for computing the Discrete Fourier Transform . This method was applied for the estimation of all spectra and so will be described in greater detail in subsequent sections of this chapter .

Recently Akaike (1969, 1970) and Parzen (1968) have argued in favour of estimating $S_{xx}(f)$ by autoregressive decomposition . Samples $x(n)$ of the time series are assumed to have the form :

$$x(n) = \sum_{p=0}^{\infty} c_p \; e(n-1)$$

where $c_0 = 1$ and the $e(n)$'s are completely uncorrelated . With this assumption $x(n)$ can be approximated by

$$x(n) \tilde{=} e(n) + \sum_{m=1}^{p} a_{p,m} \; x(n-m)$$

and if $x(n)$ is a realization of a weakly stationary process this approximation is stable and can be made as accurate as desired by increasing p . The magnitude of p can be estimated from the auto-covariance function estimate . From estimates of the auto-regressive coefficients $a_{p,m}$ an auto-regressive estimator of the normalized sample spectrum may be obtained . It has been claimed (Gersch, 1970) that this method gives smoother spectra which are more readily interpretable than spectral estimates obtained by the Blackman- Tukey method or the direct method , and that this method is more objective. However, this method has as yet found little application . It appears to be better suited for the estimation of the spectra of noisy

signals than for estimating spectra of random signals and spike trains in order to estimate frequency resonse functions or coherence functions .

3.4. Sampling a continuous signal .

The computation of estimates of $S_{xx}(f)$ on a digital computer implies that in place of the continuous parameter process $\{ x(t) , -\infty < t < \infty \}$ one must use a discrete parameter process $\{ x_{(\Delta t)}(n) : n = 0, \pm 1, \pm 2... \}$ which may be formed by setting

$$x_{(\Delta t)}(n) = x(n\Delta t)$$

choice of Δt follows from the Nyquist sampling theorem (Nyquist, 1928 ; Landau, 1967) . If x(t) is a signal of finite energy bandlimited to B hz. i.e.

$$x(t) = \sum_{-\infty}^{\infty} a_k \left\{ \frac{\sin 2\pi B(t - k/2B)}{2\pi B(t - k/2B)} \right\} \qquad 3.9$$

with $\Sigma |a_k|^2 < \infty$

then x(t) can only be recovered error-free from $x_{(\Delta t)}(n)$ if

$$1/\Delta t > 2B$$

Half the sampling rate , $1/ 2\Delta t$, is called the Nyquist or folding frequency f_N. If x(t) has a spectrum $S_{xx}(f)$, then it can be shown (Blackman and Tukey, 1958) that $S_{xxA}(f)$, the spectrum of $x_{(\Delta t)}(n)$ is given by

$$S_{xxA}(f) = S_{xx}(f) + \sum_{k=1}^{\infty} [S_{xx}(2kf_N - f) + S_{xx}(2kf_N + f)] \qquad 3.10$$

Thus if there is any power in $S_{xx}(f)$ for $f > f_N$ this power will alias as power at frequencies $f < f_N$. The only method of preventing such aliasing when taking regular samples is to choose Δt such that $f_N >$ all f_i where $S_{xx}(f_i) \neq 0$. This may be simply achieved by filtering $x(t)$ before sampling , and choosing an appropriate Δt. When Δt is such that the regular samples are alias-free , recovery of $x(t)$ from $x_{(\Delta t)}(n)$ is stable , that is , small errors such as quantizing errors (Gold and Rader, 1969) in the samples $x_{(\Delta t)}(n)$ give small errors in the recovered $x(t)$ and hence in estimates of $S_{xx}(f)$.

A variety of methods for alias-free sampling of a stochastic process have been proposed in which the sampling times t_i are random (Beutler, 1970) . When the sampling times form a Poisson process , or are obtained by random deletions from a regular process ,alias-free sampling can be achieved at mean sampling rates less than the Nyquist rate . However such techniques are not readily implementable .

3.5. Sampling a spike train.

A recorded spike train is a band-limited signal of finite energy as defined by equation 3.9 , but since the duration of action potentials is of the order of milliseconds regular alias-free samples would have to have an excessively high sampling rate . A variety of methods have been proposed for sampling a spike train , and these have been criticized elsewhere (French and Holden, 1971a) together with a full description of a new method for obtaining alias-free samples of a spike train .

In the method used to obtain alias-free regular samples of a spike train the spike train is treated as a stochastic point process . Bartlett (1963) has defined the periodogram (see section 3.7) of a stochastic

point process as the Fourier Transform of dn(t) , where dn(t) is the differential of the cumulative distribution function n(t) . n(t) of any point process is a staircase function , with jump discontinuities of unity height at the occurance times of the events . Thus dn(t) is a series of unit impulses or Dirac delta functions at the occurance times t_i of the events . An alternative justification for treating a spike train as a series of unit impulses is given by Nelsen (1964) . Thus treatment of a spike train as a stochastic point process is identical to treatment as a series of unit impulses given by

$$y(t) = \sum_{i=1}^{\infty} \delta(t - t_i) \qquad 3.11$$

in order to estimate the periodogram .

The spectrum of a series of unit impulses extends to an arbitrarily high frequency, so $S_{yy}(f) > 0$ for $0 < f < \infty$, and so unless the impulse train is filtered aliasing will be unavoidable . Among the advantages of digital filters over analog filters is that a digital filter can have an impulse response which exists for negative times . Figure 3.4 shows the filter characteristics of an ideal , rectangular low pass filter , and its impulse response , which is given by

$$g(t) = f_N [\sin(2\pi f_N t)]/2\pi f_N t \qquad 3.12$$

$$- \infty < t < \infty$$

Such a filter may only be generated digitally .

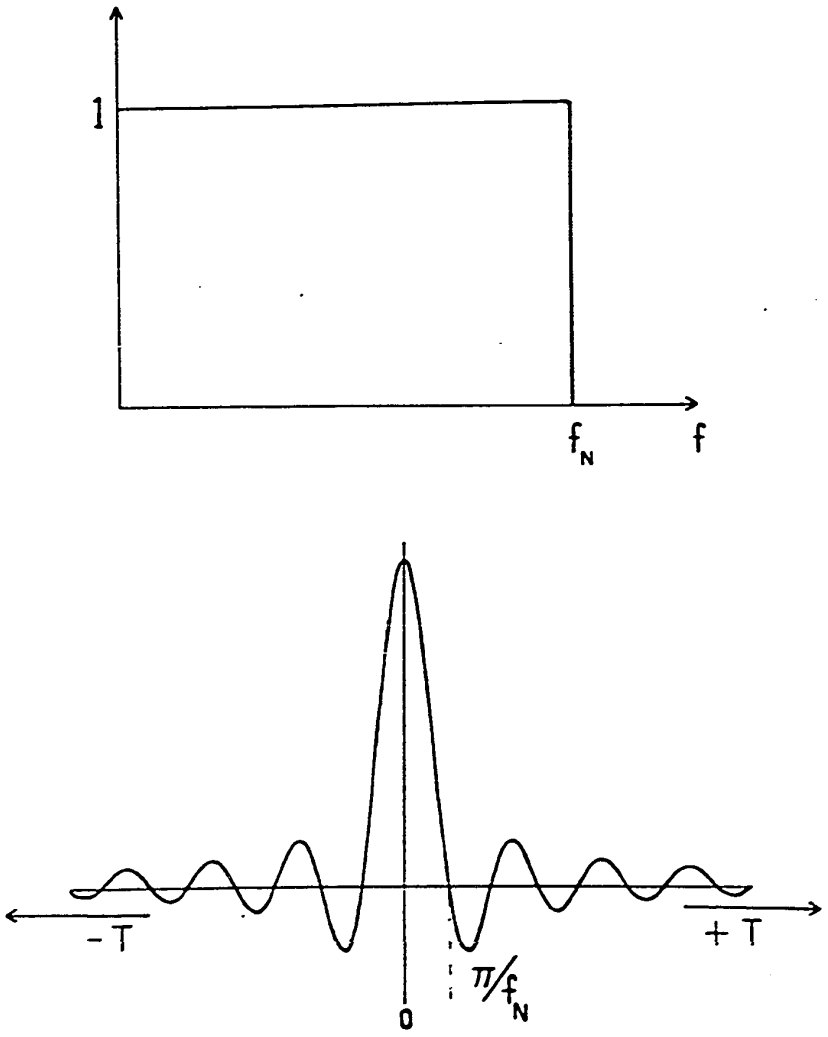

Figure 3.4 . Ideal , rectangular low-pass filter and its impulse response .

Thus the series of delta functions of equation 3.11 may be digitally filtered by convolving each unit impulse with $g(t)$. Implementation of this technique may be considered conceptually as a sequence :

i). $$y_T(t) = \begin{cases} y(t) & 0 < t < T \\ 0 & t > T \end{cases}$$

ii). each unit impulse at t_i is convolved with $g(t)$ to give a function $y'(t)$ for $-\infty \leqslant t \leqslant \infty$

iii). $$y'_T(t) = \begin{cases} y'(t) & 0 < t < T \\ 0 & t > T \end{cases}$$

iv).

$$y'_{T(\Delta t)}(n) = y'_T(n\Delta t)$$

Thus the result is equispaced samples of the digitally filtered train of unit impulses , and where $f_N = 1/2\Delta t$ these samples are alias-free . Details of practical aspects of the implementation of this technique are given in French and Holden (1972).

3.6. The Discrete and Fast Fourier Transforms .

The sampling methods of sections 3.4 and 3.5 generate from $x_T(t)$ and $y_T(t)$ a series of N numbers , $x_{T(\Delta t)}(n)$ and $y_{T(\Delta t)}(n)$ for $n = 0, 1, \ldots N-1$. The Fourier Transform of such sets of numbers may not be defined . However , a discrete set of numbers may be associated with a time function

$$x'(t) = \sum_{n=0}^{N-1} x(n\Delta t) \quad \delta(t - n\Delta t)$$

whose Fourier Transform is given by

$$X'(f) = \int_{-\infty}^{\infty} x'(t)\, e^{-j2\pi ft}\, dt$$

$$= \sum_{n=0}^{N-1} x(n\Delta t)\, e^{-j2\pi f\Delta t} \qquad 3.13$$

This method of obtaining the Fourier Transform of $x(n\Delta t)$ provides a means of defining the Discrete Fourier Transform of a set of N numbers $x(n)$, $n = 0, 1, \ldots. N-1$ as

$$X(m) = \sum_{n=0}^{N-1} x(n)\, e^{-j2\pi nm/N} \qquad 3.14$$

and the inverse transform by

$$x(n) = \frac{1}{N} \sum_{m=0}^{N-1} X(m)\, e^{j2\pi nm/N} \qquad 3.15$$

Thus the sequences $x(n)$ and $X(m)$ which form a Discrete Fourier Transform pair are periodic , with a period N . This may be visualized by considering $x(n)$ and $X(m)$ to be defined at integer points on a circle of circumference N (Cooley,Lewis and Welch, 1969 ; Gold and Rader, 1969) . Thus the Discrete Fourier Transform is not simply a discrete

analog of the Fourier Transform , but has some properties of its own .

The Fast Fourier Transform , rediscovered by Cooley and Tukey (1965) , is an algorithm for the efficient evaluation of the Discrete Fourier Transform similar to that described by Danielson and Lanczos (1942) . The evaluation of equation 3.14 requires N^2 complex multiplications and divisions , and so until the rediscovery of the Fast Fourier Transform the indirect method of estimating spectra was computationally more efficient than the direct method when N was large . There are two kinds of Fast Fourier Transform algorithm , decimation in time (Cooley and Tukey , 1965) and decimation in frequency (Gentleman and Sande, 1966) . Both of these algorithms result in the reduction in the number of operations needed to compute an N point transform from N^2 to $N \log_2 N$ when N is an integral power of 2 . As well as the saving in computing time it has been claimed that the Fast Fourier Transform is more accurate than the Discrete Fourier Transform since the smaller number of operations produce fewer round-off errors (Wienstein, 1969) .

3.7. Consistent spectral estimation by the direct method .

If $x(n) : n = 0, 1, \ldots, N-1$ are N alias-free samples of $x(t)$ taken at regular intervals Δt from a record of length $T = N\Delta t$ application of equation 3.14 gives the Fourier coefficients of $x(n\Delta t)$, $X(m\Delta f)$. These Fourier coefficients are complex and so

$$X(m\Delta f) = A_{m/} + jB_{m/}$$

where the index Δf has been omitted for clarity in subsequent equations. The Fourier coefficients occur at equally spaced points with a frequency resolution of $1/N\Delta t$.

An estimate of the spectrum , the periodogram $I_{xx}(m\Delta f)$ is given by

$$I_{xx}(m\Delta f) = \frac{X(m\Delta f)\, X^*(m\Delta f)}{N}$$

$$= \frac{|\, X(m\Delta f)|^{\,2}}{N}$$

$$= \frac{1}{N}\left[\, A_m^{\,2} + B_m^{\,2}\,\right] \qquad 3.16$$

The periodogram is purely real and as it is an even function only $[\, N/2\,] + 1$ values are distinct . It is not a good estimate of the spectrum $S_{xx}(f)$ since it is biased and is not consistent . The bias occurs since the time series has been viewed through a rectangular data window of width T , and so the coefficients have been convolved with $T\,[\, \sin \pi fT\,]/\, \pi fT$, and so the periodogram is given by

$$I_{xx}(m\Delta f) = \int_{-\infty}^{\infty} T \left[\frac{\sin \pi f'T}{\pi fT}\right]^2 S_{xx}(f-f')\, df' \qquad 3.17$$

where $T\,[\, \sin \pi f'T/\, \pi f'T\,]^2$ is the Bartlett spectral window.

In the case where x(t) is a spike train which does not have a constant interspike interval $S_{xx}(0) >> S_{xx}(f \neq 0)$, and so this convolution will produce massive leakage from the DC component . This DC leakage is often a problem and so is always eliminated by generating from $x(n) : n = 0, 1, .. ,N-1$ a series with a zero mean and hence no DC component .

However , there will still be bias if the spectrum $S_{xx}(f)$ is not smooth . This bias due to leakage may be reduced by linear modification of the Fourier coefficients - a simple and widespread method is Hanning , in which the Fourier coefficients are convolved with - 1/4 , + 1/2 and -1/4 so that

$$\begin{aligned} A_0 &= 1/2 \, [\, A_1 + A_0 \,] \\ A_m &= -(1/4)A_{m-1} + (1/2)A_m - (1/4)A_{m+1} \\ A_{N-1} &= 1/2 \, [\, A_{N-1} + A_{N-2} \,] \end{aligned} \qquad 3.18$$

and similarly for the B_m . Convolution of the Fourier coefficients with these Hanning weights is equivalent to viewing the time samples through a cosine bell $w_h(n)$ given by

$$w_h(n) = \frac{1}{2} \left[1 - \cos \frac{2\pi n}{N-1} \right]$$

A disadvantage of linear modification is that it results in a decrease in frequency resolution with only a small decrease in variance . Quadratic modification , convolving ($A_m^2 + B_m^2$) with an apparently suitable spectral window , has little effect on leakage (Bingham, Godfrey and Tukey , 1967 ; Sloane, 1969) but does permit the trading of a decrease in frequency resolution for a decrease in variance .

Obtaining a zero-mean series and Hanning can reduce bias due to leakage , but the linearly modified periodogram is not a consistent estimator of the spectrum . If x(n) are samples from a Normal process ,

since the Fourier Transform is a linear transformation A_m and B_m will be Normally distributed and so $I_{xx}(m\Delta f)$ will have a chi-squared distribution with two degrees of freedom . If x(n) are samples from a process which does not have a Normal distribution but N is large then from the Central Limit Theorem A_m and B_m will have approximately Normal distributions and so $I_{xx}(m\Delta f)$ will have approximately a chi-squared distribution with two degrees of freedom . The expected value of $I_{xx}(m\Delta f)$ is

$$E\ \{\ I_{xx}(m\Delta f)\ \} = \int_{-\infty}^{\infty} T\left[\frac{\sin \pi f' T}{\pi f' T}\right]\ S_{xx}(f-f')\ df' \qquad 3.19$$

and the variance is approximately $S_{xx}^2(f)$.

If

$$W(m) = \sum_{n=0}^{N-1} w_h(n)\ e^{-j2\pi nm/N} \qquad 3.20$$

where $w_h(n)$ is the Hanning window then the expected value of the linearly modified periodogram $\hat{I}_{xx}(m\Delta f)$ is

$$E\ \{\ \hat{I}_{xx}(m\Delta f)\} = \frac{2\ E\{\ X(m)^2\}}{N}\ \Sigma\ W(m)^2 \qquad 3.21$$

and the variance

$$\text{Var}\ \{\ \hat{I}_{xx}(m\Delta f)\} = \frac{4\ E^2\{\ X(m)^2\}}{N^2}\ [\ W(m)^2\ ]^2 \qquad 3.22$$

hence

$$\text{Var}\ \{\hat{I}_{xx}(m\Delta f)\} = E^2\ \{\ \hat{I}_{xx}(m\Delta f)\}$$

as in the case of the unmodified periodogram (Jenkins and Watts, 1968) .

The variance of the modified periodogram $\hat{I}_{xx}(m\Delta f)$ may be reduced by averaging M periodogram estimates from non-overlapping records of length T . The variance of the averaged modified periodogram $\tilde{\hat{I}}_{xx}(m\Delta f)$ is now approximately

$$\frac{1}{M} \; S^2_{xx}(f)$$

and the averaged , modified periodogram has approximately a chi-squared distribution with 2M degrees of freedom . A further decrease in variance to 55% can be achieved by having the record segments overlap by T/2 (Welch, 1967) . If the resolution of $\tilde{\hat{I}}_{xx}(m\Delta f)$ is unnecessarily fine a further reduction in variance can be achieved by averaging adjacent frequency components (Jones, 1965) .

When k is the number of effective degrees of freedom of the averaged estimate of the modified periodogram Jenkins and Watts have shown that 100(1 - α)% confidence limits for the estimate are given by

$$\frac{k \; \tilde{\hat{I}}_{xx}(m\Delta f)}{z_k(1 - \alpha/2)} < S_{xx}(m\Delta f) < \frac{k \; \tilde{\hat{I}}_{xx}(m\Delta f)}{z_k(\alpha/2)}$$

where $z_k(1 - \alpha/2)$ and $z_k(\alpha/2)$ are the $\alpha/2$ and $1 - \alpha/2$ points on the cumulative chi-squared distribution with k degrees of freedom as given in Bendat and Piersol (1966) .

3.8. Consistent cross-spectral estimation by the direct method .

The sample cross-spectrum is defined by

$$S_{xy}(f) = \frac{1}{T} X_T^*(f)\, Y_T(f) \qquad 3.24$$

$$= \frac{1}{T} [A_x(f) - jB_x(f)]\, [A_y(f) + jB_y(f)]$$

where $[A_x(f) + jB_x(f)]$ and $[A_y(f) + jB_y(f)]$ are the Fourier Transforms of $x_T(t)$ and $y_T(t)$. Estimation of the cross-spectrum by the cross-periodogram $\tilde{\hat{I}}_{xy}(m\Delta f)$ is analogous to the estimation of $S_{xx}(f)$ by $\tilde{\hat{I}}_{xx}(m\Delta f)$: the record is broken into subrecords of length T , and for each subrecord $\frac{1}{T} X_T^*(m\Delta f)\, Y_T(m\Delta f)$ is evaluated from linearly modified Fourier coefficients , and periodograms from different subrecords are averaged to form $\tilde{\hat{I}}_{xy}(m\Delta f)$.

$\tilde{\hat{I}}_{xy}(m\Delta f)$ can be considered either in terms of its magnitude and phase

$$\tilde{\hat{I}}_{xy}(m\Delta f) = \tilde{\hat{M}}_{xy}(m\Delta f)\; e^{j\tilde{\hat{P}}_{xy}(m\Delta f)} \qquad 3.25$$

where

$$\tilde{\hat{M}}_{xy}(m\Delta f) = \left| \tilde{\hat{I}}_{xy}(m\Delta f) \right|$$

and

$$\tilde{\hat{P}}_{xy}(m\Delta f) = \tan^{-1} \frac{IM\ \tilde{\hat{I}}_{xy}(m\Delta f)}{RE\ \tilde{\hat{I}}_{xy}(m\Delta f)}$$

or in terms of its real and imaginary parts , which are estimates of the co- and quad-spectrum .

If $\tilde{\hat{I}}_{xy}(m\Delta f)$ is the average of M cross-periodogram estimates which have not been subject to linear modification then the variance

of $\tilde{\hat{M}}_{xy}(m\Delta f)$ is given by Hinich and Clay (1968) as

$$\mathrm{Var}\{\tilde{\hat{M}}_{xy}(m\Delta f)\} = \frac{1}{2M} S_{xx}(f) S_{yy}(f) [\, 1 + \gamma^2(f) \,]$$

and

$$\mathrm{Var}\{\tilde{\hat{P}}_{xy}(m\Delta f)\} = \frac{1}{2M} \left[\frac{1}{\gamma^2(f)} - 1 \right]$$

Thus the variance of the cross-spectrum estimate is dependent on the coherence function.

3.9. Consistent estimation of the coherence function .

If the coherence function defined by equation 2.22 is estimated from the linearly modified but unaveraged periodograms by

$$\gamma^2(f) = \frac{| \hat{I}_{xy}(f) |^2}{\hat{I}_{xx}(f)\ \hat{I}_{yy}(f)} \qquad 3.26$$

it will be identical with unity everywhere except when $\hat{I}_{xx}(f).\hat{I}_{yy}(f)$ is zero since if (a + jb) , (a'+ jb') are the Fourier coefficients of $x_T(t)$ and $y_T(t)$

$$\frac{| I_{xy}(f)|^2}{I_{xx}(f).\ I_{yy}(f)} = \frac{\left| \frac{(a - jb)(a' + jb')}{T} \right|^2}{\frac{(a - jb)(a + jb)}{T} \ \frac{(a'-jb')(a'+jb')}{T}}$$

$$= 1 .$$

Thus equation 3.26 is a useless estimator of $\gamma^2(f)$, and it is

analogous to estimating the correlation coefficient from a single observation pair .

A widely used estimator of the coherence function is

$$\tilde{\gamma}^2(f) = \frac{| \tilde{\hat{I}}_{xy}(f) |^2}{\tilde{\hat{I}}_{xx}(f) \quad \tilde{\hat{I}}_{yy}(f)} \qquad 3.27$$

but this is a biased estimator . Enochson and Goodman (1965) have shown that estimates of the coherence function are positively biased and that this bias is a function of the effective degrees of freedom of the estimate and the true coherence , and have given curves of a bias correction factor when the true coherence is greater than 0.4 . Benignus (1969b) used Monte Carlo methods to investigate this bias and produced an empirical family of curves relating the bias to the effective degrees of freedom of the estimate and the true coherence for all values of coherence between zero and one . These curves were fitted by a least squares procedure and the estimate of bias $\hat{B}\,[\tilde{\gamma}^2(f)\,]$ is given by

$$\hat{B}\,[\,\tilde{\gamma}^2(f)\,] = \frac{1}{k}\,(\,1 - \tilde{\gamma}^2(f)\,) \qquad 3.28$$

and so that the corrected estimate of coherence is given by

$$\hat{\tilde{\gamma}}^2(f) = \tilde{\gamma}^2(f) - \hat{B}\,[\,\tilde{\gamma}^2(f)\,]$$

The residual error between $\hat{\tilde{\gamma}}^2(f)$ and $\gamma^2(f)$ was less than 0.01 for all estimates with $k > 8$.

Tick (1967) has proposed an alternative family of estimators for $\gamma^2(f)$. In place of just averaging the linearly modified periodograms he proposes that coherence function estimates obtained from averaged modified periodograms should themselves be averaged . This estimate is more biased when the true phase between the two signals is changing slowly , but is less biased when the true phase is changing rapidly . In Monte Carlo studies , where the true coherence is known , the number of periodograms averaged to be used to form a coherence function estimate , and the number of coherence function estimates to be averaged can be optimized to form an accurate estimate . However , when the true coherence is unknown this method is not very useful but does suggest that there is no optimal method for estimating an unknown coherence function .

Benignus (1969a) discussed the estimation of the coherence function by use of the Fast Fourier Transform , and favours an estimator produced by both averaging a set of periodograms and averaging over frequency segments within the periodograms . When averaging over frequency segments the adjacent components are not independent if the coefficients have been linearly modified , and so care must be taken in evaluating the effective degrees of freedom k .

Goodman (1957) has derived a distribution function for the positive square root of the coherence function between two Gaussian processes , and this has been tabulated by Amos and Koopmans (1963) . Using Monte Carlo methods Foster and Guinzy (1967) have shown that this distribution is applicable to non-Gaussian processes if the spectra $S_{xx}(f)$, $S_{yy}(f)$ and $S_{xy}(f)$ are reasonably smooth , and by using a Bayesian approach (Good, 1965) have obtained a maximum

likelihood estimator for the coherence function : however , when k is large this estimator does not differ significantly from $\hat{\gamma}^2(f)$.

Enochson and Goodman (1965) have shown that the sampling distribution of the Fisher Z-transform (Kaplan , 1962) of the positive square root of the coherence function estimate is approximately Gaussian with a variance given by

$$\text{Var} \{ Z \sqrt{\hat{\gamma}^2}(f) \} = \frac{1}{2k}$$

when $0.4 < \hat{\gamma}^2(f) < 0.95$ and $k > 20$.

Hinich and Clay (1968) have given the variance of $\sqrt{\hat{\gamma}^2}(f)$ as

$$\text{Var} \{ \sqrt{\hat{\gamma}^2}(f) \} \sim \frac{1}{2k} [1 - \sqrt{\gamma}^2(f)]^2$$

and so the variance of the coherence function estimate depends on the value of the true coherence .

Approximate confidence limits for $\hat{\gamma}^2(f)$ are given by

$$\hat{U}(f) \pm \frac{m\{ 1 - \alpha/2 \}}{\sqrt{k}} \qquad 3.29$$

wher m $\{1 - \alpha/2\}$ is the $1 - \alpha/2$ point on the cumulative unit Normal distribution function and

$$\hat{U}(f) = \tanh^{-1} \hat{\gamma}^2(f)$$

which is assumed (by appealing to the Central Limit theorem) to have

a Normal distribution (Bendat and Piersol, 1966) .

3.10. Consistent estimation of the frequency response function .

The frequency response function G(f) defined by equations 2.16 - 2.18 may be estimated from

$$\hat{G}_1(f) = \frac{\hat{\tilde{I}}_{xy}(f)}{\hat{\tilde{I}}_{xx}(f)} \qquad 3.30$$

or

$$\hat{G}_2(f) = \frac{\hat{\tilde{I}}_{yy}(f)}{\hat{\tilde{I}}_{yx}(f)} \qquad 3.31$$

Note that

$$\frac{\hat{G}_1(f)}{\hat{G}_2(f)} = \hat{\tilde{\gamma}}^2(f)$$

and so these two estimates will only be the same if the coherence function is one . Bendat (1962) has argued that $\hat{G}_1(f)$ should be used to estimate G(f) when the output is contaminated with noise , and $\hat{G}_2(f)$ should be used when the input measurement system introduces noise . $\hat{G}_1(f)$ was used to estimate G(f) since the coherence function was never one.

$\hat{G}(f)$ is complex , and confidence limits for its magnitude $|\hat{G}(f)|$ and phase $\underline{/}\hat{G}(f)$ are given by Jenkins and Watts (1968) as

$$| \hat{G}(f) | \left[1 \pm \left\{ \frac{2}{k-2} f_{2,k-2}\{1-\alpha\} \frac{1-\hat{\gamma}^2(f)}{\hat{\gamma}^2(f)} \right\}^{1/2} \right] \quad 3.32$$

and

$$\underline{/}\hat{G}(f) \pm \left[\sin^{-1} \frac{2}{k-2} f_{2,k-2}\{1-\alpha\} \frac{1-\hat{\gamma}^2(f)}{\hat{\gamma}^2(f)} \right]^{1/2} \quad 3.33$$

where $f_{2,k-2}$ is the $1-\alpha$ point on the cumulative Fisher's F distribution with 2 degrees of freedom and $k-2$ degrees of freedom .

The variance of $| \hat{G}(f) |$ and $\underline{/}\hat{G}(f)$ are given by

$$\mathrm{Var}\{ | \hat{G}(f) | \} \sim \frac{G(f)}{2k} \left[\frac{1}{\gamma^2(f)} - 1 \right]$$

and

$$\mathrm{Var} \{ \underline{/}\hat{G}(f)\} \sim \frac{1}{2k} \left[\frac{1}{\gamma^2(f)} - 1 \right]$$

and so for low values of coherence the variance is high .

3.11. Software for spectral estimation .

The input signals were sampled using SAP-1 (II) (French and Holden, 1972) and the Fourier coefficients obtained by SAP-3 which utilizes a time decimation Fast Fourier Transform algorithm (French and Holden, 1971b) . Hanned spectral estimates were obtained from the Fourier coefficients and averaged by SAP-9 (French, 1971) and estimates of the spectra , frequency response functions , coherence function and information transmission rate and their confidence

limits were generated by FOCAL programs accessing the stored spectral estimates by SAP-4 (French and Holden, 1971b) .

A flow chart showing the principal computational routes is given in Figure 3.5 . A full discussion of computational aspects of spectral estimation by the Fast Fourier Transform are given in Cooley, Lewis and Welch (1967) and Brumbach (1968) .

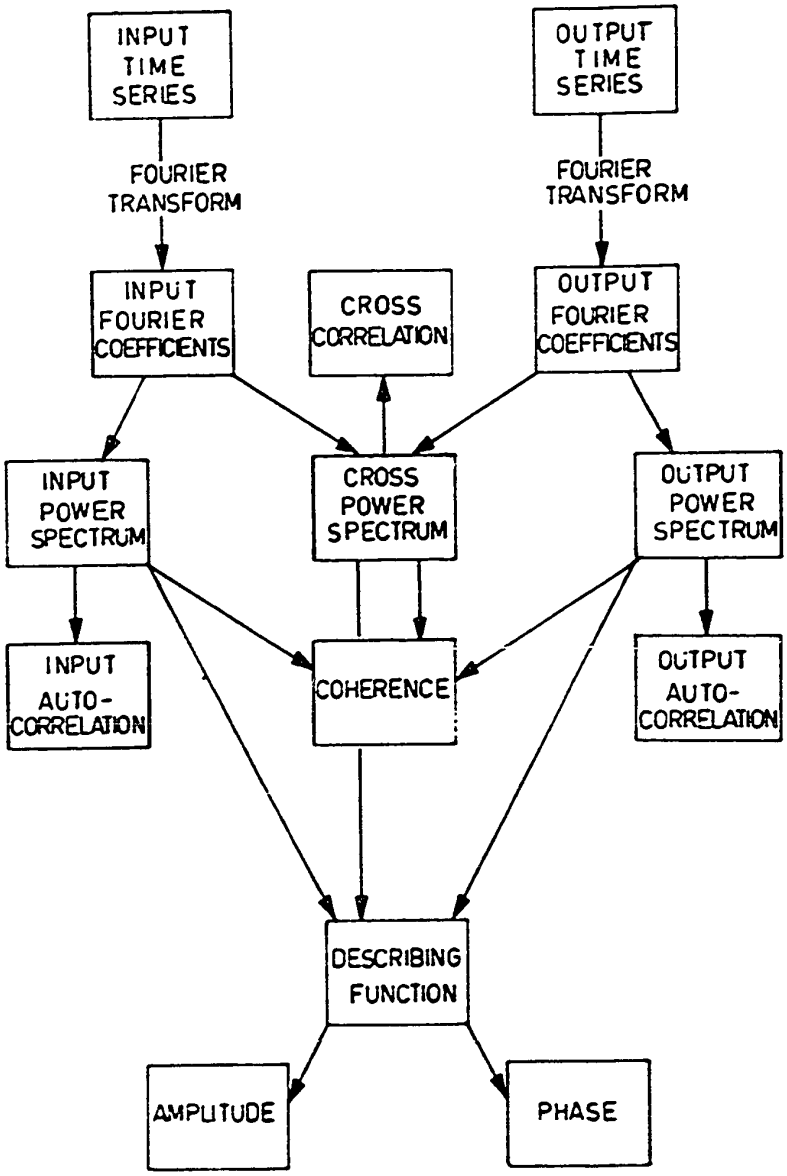

Figure 3.5 . Flow chart of principal computation routes of spectral analysis package .

CHAPTER 4 .

THE COCKROACH TACTILE SPINE .

4.1. Introduction .

Pringle and Wilson (1952) utilized linear systems theory to obtain a quantitative model for the input-output relations of the large tactile spine on the dorsal surface of the femur of the meta-thoracic leg of the cockroach , Periplaneta americana . Sinusoidal and rectangular wave driving functions were applied to the receptor , and a 'transfer function' relating the input tension to the rate of sensory spike discharge was obtained . This receptor has been studied using a wide variety of techniques (Chapman and Smith , 1963 ; Crowe, 1967 ; Pearson and Holden, 1970 ; Holden and French, 1971a , 1971b ; French, Holden and Stein, 1972) and thus it provides a very convenient preparation for the development and comparison of different techniques of analysis .

Pringle and Wilson took the rate of sensory spikes as the output from the receptor , and fitted the response to a square wave tension driving function by the linear sum of three decaying exponential functions . This would give a frequency response function which would have in phase modulation at low frequencies , and an increasing sensitivity and phase lead passing through local maxima with increasing frequency . However , a range of sinusoidal driving functions adequate to test this model was not available .

Chapman and Smith (1963) re-examined the preparation using similar driving functions , and fitted the rectangular wave response by a power function decay . The frequency response function predicted from this response has a constant phase lead and the sensitivity increases as a power of the forcing frequency . This frequency response function was supported by the use of sinusoidal driving functions with frequencies from 0.1 to 10hz. .

Crowe (1967) compared the response predicted by both models in response to ramp driving functions with the experimentally observed response , and his results tended to support Pringle and Wilson's model .

This lack of agreement suggests that the frequency response function of this receptor should be estimated using a number of techniques and the results compared . If the system is non-linear an estimate of the frequency response function based on one kind of driving function may not necessarily predict the response to other driving functions .

4.2. Methods .

All experiments were performed on the single large tactile spine located on the dorsal surface of the end of the femur of either metathoracic leg of adult cockroaches , Periplaneta americana . The leg was cut through at the coxa , and the cut surface covered with Vaseline to prevent drying . The leg was mounted on the armature of a Pye-Ling vibration generator (three ohm input impedance , model V47) by two insect pins on a piece of cork , and the pins served as recording electrodes . This simple recording method is effective because of

the high resistance of the narrow femur and since each spine is innervated by a single axon (Chapman and Nichols, 1969) .

The vibration generator was driven by the output from a force servo control unit via a power amplifier (for impedance matching) . The feedback transducer to the servo was the differential output from two Endevco Laboratories Pixie 8101 force transducers . The differential output was taken in order to compensate for temperature dependent DC shifts . The transducers respond linearly up to 40 gms.-wt. , however , the addition of a lever extension limited this range to 5 gms.-wt. . The extension of the force transducer was held against the spine . The command signal to the servo could be :

i). the output from a Hewlett-Packard 3300A function generator which had passed through a calibrated amplitude and offset control unit

ii). the output from a band-limited white noise generator

iii). any linear sum of (i) and (ii) above .

The amplified action potentials , the output from the force transducer and reference markers were recorded on a Thermionic Products T3000 FM tape recorder for subsequent processing on the LAB-8 computer .

Estimates of the frequency response function were obtained by subjecting the tension servo which stimulated the receptor to

a) deterministic driving functions (sinusoids and rectangular waves)

b) sinusoidal driving functions added to a band-limited white noise auxiliary signal

c) band-limited white noise .

Cycle histograms of the response to deterministic sinusoidal

driving functions were fitted using a least mean squares procedure (Sokolnikoff and Redheffer, 1958) . When band-limited white noise was the driving function the input , output and cross-spectra were estimated . The algorithms and programming methods used have been described elsewhere (French, 1970 ; French and Holden, 1971a ; 1971b ; 1972) .

4.3. Results .

The cycle histograms in response to a 0.05 hz. rectangular wave driving function of two different amplitudes are shown in Figure 4.1. These histograms could not be fitted by a single decaying exponential function . The best-fitting (in the sense of least mean squared deviation) exponential decayed slower than the histogram in the first second and faster than the histogram in the last few seconds . The histogram could be fitted by the sum of several exponentials using a method of successive approximations , however this was not reproducible . A log-log plot of the histogram (insert on Figure 4.1) could be fitted by a straight line , with a slope of 0.82 ± 0.03 and a linear correlation coefficient of 0.80 ± 0.01 for fourteen different spines . This implies that the histogram may be fitted by a power function decay of the form

$$y(t) = b\, t^{-k} \qquad 4.1$$

where y(t) is the number of spikes/second and k is a constant given by the slope of the log-log plot . Although minimizing mean squared error on a log-log plot does not necessarily minimize mean squared

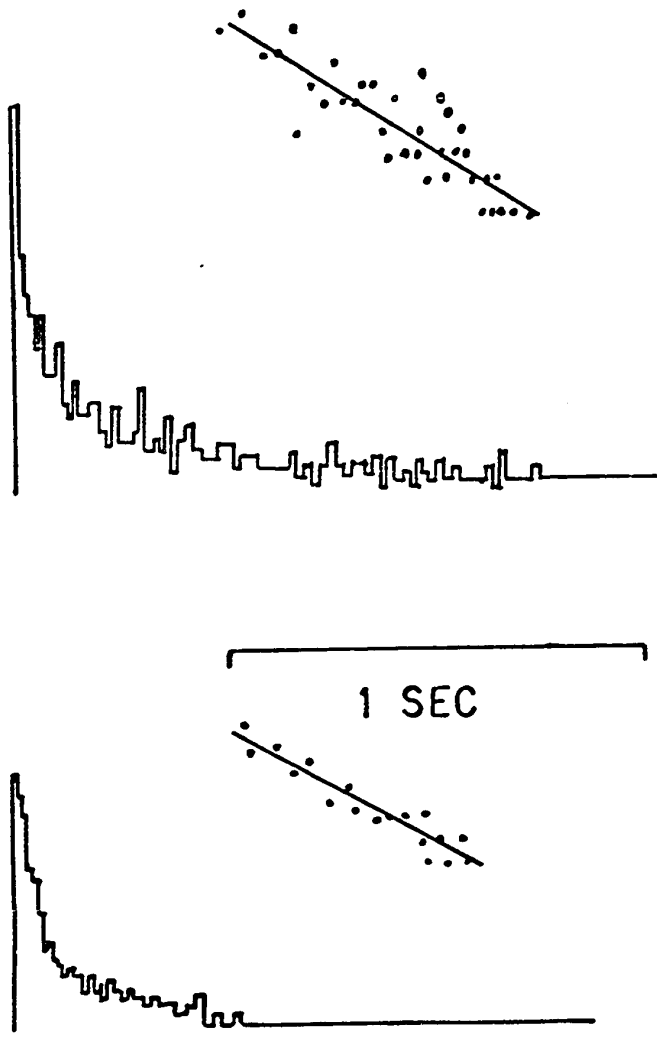

Figure 4.1 . Cycle histograms of the response of a tactile spine to a 0.05 hz. rectangular driving function of two different amplitudes . Inserts show log-log plots .

error on the linear plot of the histogram the computed curve fits the histogram well .

This step response is similar to that given by Chapman and Smith (1963) for the decay of instantaneous spike rate . The describing function predicted from such a step response is given by

$$H(f) = b\,\Gamma(1-k)\,f^{k}\,e^{jk\pi/2} \qquad 4.2$$

where Γ is the gamma function defined by

$$\Gamma(x) = \int_0^{\infty} u^{x-1} e^{-u}\,du \qquad 4.3$$

$$x > 0$$

This describing function has a constant phase advance of $k\pi/2$ radians and the sensitivity of the receptor increasing as the k^{th} power of the driving frequency .

The cycle histogram of the response to a one hz. sinusoidal driving function is not a sinusoid - Figure 4.2 shows it to be a clipped , distorted sinusoid . Hence the relation between the tension driving function and the cycle histogram is nonlinear . This may be further illustrated by plotting the Fourier coefficients of the cycle histogram . A linear system would only have a significant component at the driving frequency (assuming that there was no output in the absence of an input) . In fact there is considerable harmonic distortion , for where harmonic distortion is defined by

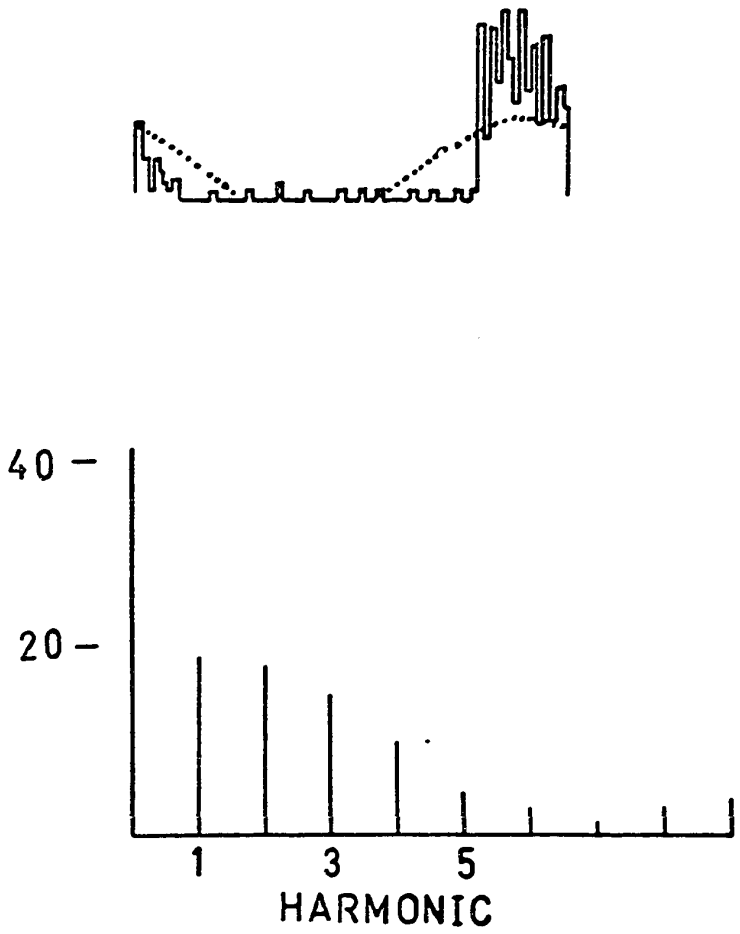

Figure 4.2 . Cycle histogram of the response of a tactile spine to a 1 hz. sinusoidal driving function and a plot of the harmonic Fourier coefficients of the histogram .

$$D_{harm} = \frac{\left[\sum_{n=2}^{6} a_n^2 + b_n^2 \right]^{1/2}}{\left[a_1^2 + b_1^2 \right]^{1/2}}$$

where a_n and b_n are the real and imaginary Fourier coefficients at a frequency n times the driving frequency , the harmonic distortion is always greater than one . The presence of appreciable first (n = 2) and third (n = 4) harmonics in Figure 4.2 is compatible with a major nonlinearity being that of rectification .

However , the amplitude of the component at the fundemental , and the amplitude of the harmonics , increase linearly with the amplitude of the sinusoidal driving function at this frequency . This linear relationship , shown in Figure 4.3 , is compatible with Crowe's (1967) observation that the maximum instantaneous rate of action potentials was linearly related to the peak to peak tension of the driving function at several low frequencies of sinusoidal driving functions . Figure 4.3 is similar to that observed with an electronic neuronal analog (French and Stein, 1970b) in the range of input amplitudes which produce rectification (Stein, French and Holden, 1972) . This linear relationship provides a justification for estimating the frequency response function by fitting the cycle histograms in response to sinusoidal driving functions by the best-fitting sine wave with a frequency equal to the frequency of the driving function . The amplitude of the best-fitting sine is $\sqrt{[a_1^2 + b_1^2]}$, a measure of the power at the driving frequency , not the peak to peak amplitude which has been widely used (Borsellino, Poppele and Terzuolo , 1965 ;

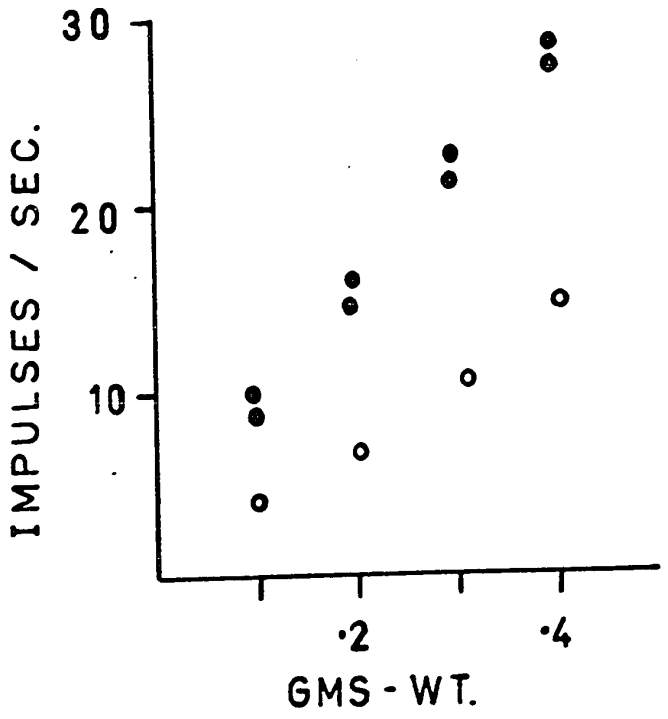

Figure 4.3 . Amplitude of the fundemental (filled circles) and the first harmonic (open circles) of cycle histograms of the response of the tactile spine to simusoidal driving functions of increasing amplitude .

Melvill Jones and Milsum, 1970) . A plot of the logarithm of the amplitude , and the phase of the fitted sine curve both as a function of the logarithm of the driving frequency form a Bode plot which characterizes the frequency response function of the receptor (D'Azzo and Houpis , 1966) .

The cycle histograms in response to sinusoidal driving functions at higher frequencies exhibit phase locking - the action potentials are entrained to specific phases of the driving function . Figure 4.4 shows the cycle histograms in response to sinusoidal driving functions at 5hz. and 20 hz. . At 5hz. there is a strong tendency for there to be five spikes/cycle occuring at phases fixed relative to the driving function , and at 20 hz. there is one-to-one phase locking . Phase locking has been observed in a variety of sensory neurones (Kiang et al. , 1965 ; Matthews and Stein, 1969a) and in simple neuronal models (Rescigno et al. , 1969 ; Stein, French and Holden, 1972) . For frequencies where one-to-one entrainment occurs the amplitude of the fitted sine curve will be twice the driving frequency .

A Bode plot of the frequency response function obtained by using sinusoidal driving functions is given in Figure 4.5 , and is compared with the frequency response function predicted from the step response of Figure 4.1 by equation 4.2 . The agreement between the predicted curve (solid line) and the data points is good up to 10hz. , above which the slope of the sensitivity curve obtained by the sine-fit method is less than that predicted from the step response . This is to be expected as phase locking occurs at frequencies above 10 hz. .

Thus the use of deterministic input signals shows two kinds of

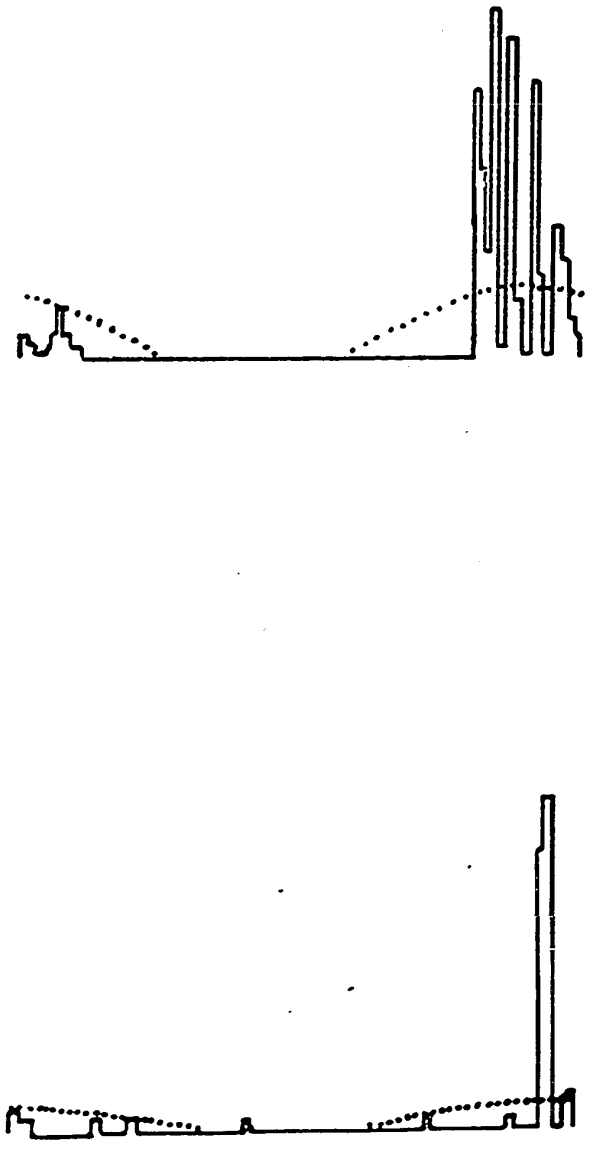

Figure 4.4 . Cycle histograms of the response of the tactile spine to 5 hz. and 20 hz. sinusoidal driving functions showing phase locking .

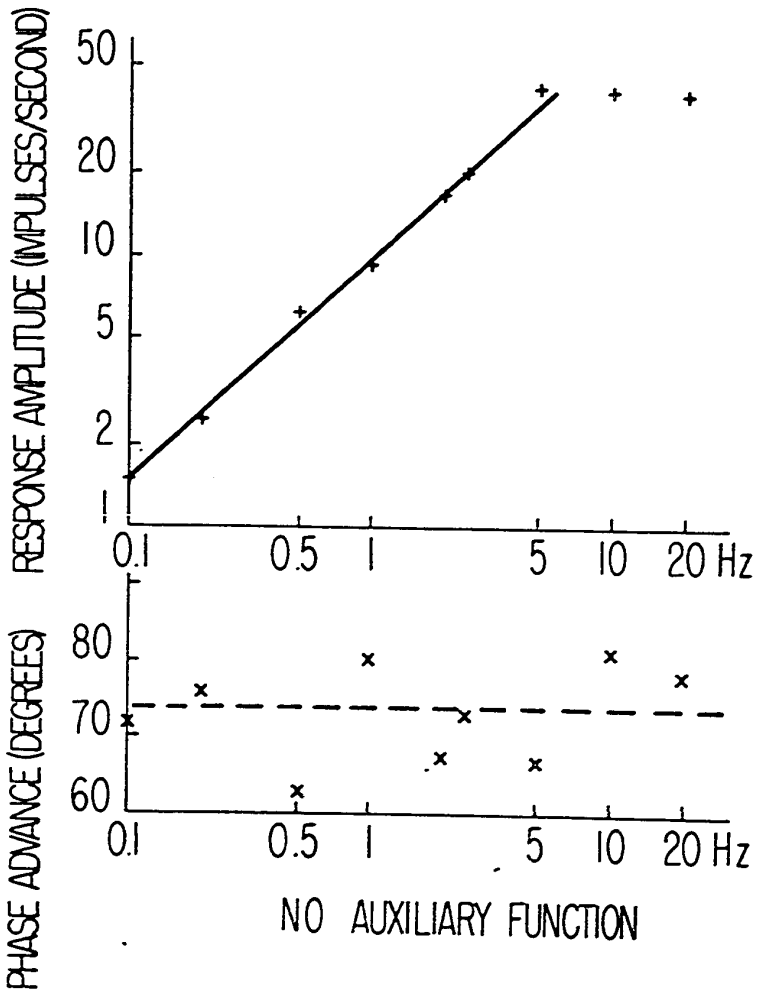

Figure 4.5 . Bode plot of the frequency response function of the tactile spine obtained by using sinusoidal driving functions .

nonlinearity when the cycle histogram is taken as the output - rectification at all frequencies and phase locking at high frequencies . From the cycle histogram in response to sinusoidal driving functions the harmonic distortion can be measured , however this is not a good estimate of the linearity of the system as no consideration is taken of nonharmonic distortion . Bayly (1968) has shown that even in the case of a perfect or linear voltage to rate convertor there is appreciable nonharmonic distortion even with small input signals . Such nonharmonic terms may not be recovered from the cycle histogram , as for a driving function with a period T the cycle histogram is viewed through a spectral window of shape $\sin(\pi fT)/\pi fT$ as illustrated in Figure 3.3 when $T = 2W$. This leakage from the coefficients will bias estimates of coefficients at all other frequencies except the harmonics . Estimates of the coefficients at the fundemental and the harmonics will not be biased by leakage from nonharmonic coefficients as building up a cycle histogram has the effect of averaging out any coefficients which do not have a constant phase relation with the driving function .

Rectification occurs in the cycle histogram since there is no carrier rate of spikes which can be modulated . Rectification can also occur when there is a carrier rate but the driving function has a large amplitude (Melvill Jones and Milsum, 1970 ; Stein, French and Holden, 1972) . If there is a carrier rate , rectification and its concomitant distortions can be avoided by use of small input signals , and so in this case rectification is a smooth static nonlinearity . However , for the case of a zero carrier rate reduction of the input amplitude does not lead to a reduction in the

harmonic content of the response , and so in this case rectification is an essential or 'hard' nonlinearity . Spekreijse and Oostings (1969) have shown that the relative harmonic content may be reduced by the addition to the driving function of an auxiliary signal which is not correlated with the driving function and then averaging the response . This method of linearization by the use of an auxiliary signal can be used to determine the order of nonlinear elements in a system and has been applied to the analysis of visually evoked responses in man (van der Tweel and Spekreijse, 1969) , retinal ganglion cell activity (Spekreijse , 1969) and insect mechanoreceptors (Pearson and Holden, 1970) .

Cycle histograms of the response of the receptor to sinusoidal driving functions added to band-limited white noise as an auxiliary signal are compared in Figure 4.6 with the cycle histograms in response to sinusoidal driving functions . The histograms with the auxiliary signal appear sinusoidal and show neither the rectification nor the phase locking apparent at the same driving frequency when there is no auxiliary signal . The auxiliary signal , which is not correlated with the driving function , may be considered to provide a random carrier rate of spike discharge which is modulated by the driving function . A Bode plot obtained by fitting cycle histograms of the response to sinusoidal driving functions in the presence of an auxiliary signal is given in Figure 4.7 . The solid lines are the frequency response curve predicted from the step response of Figure 4.1 . The data points agree with the predicted frequency response function over a wider range of frequencies than do the points of Figure 4.5 . This is because the auxiliary signal has broken the phase

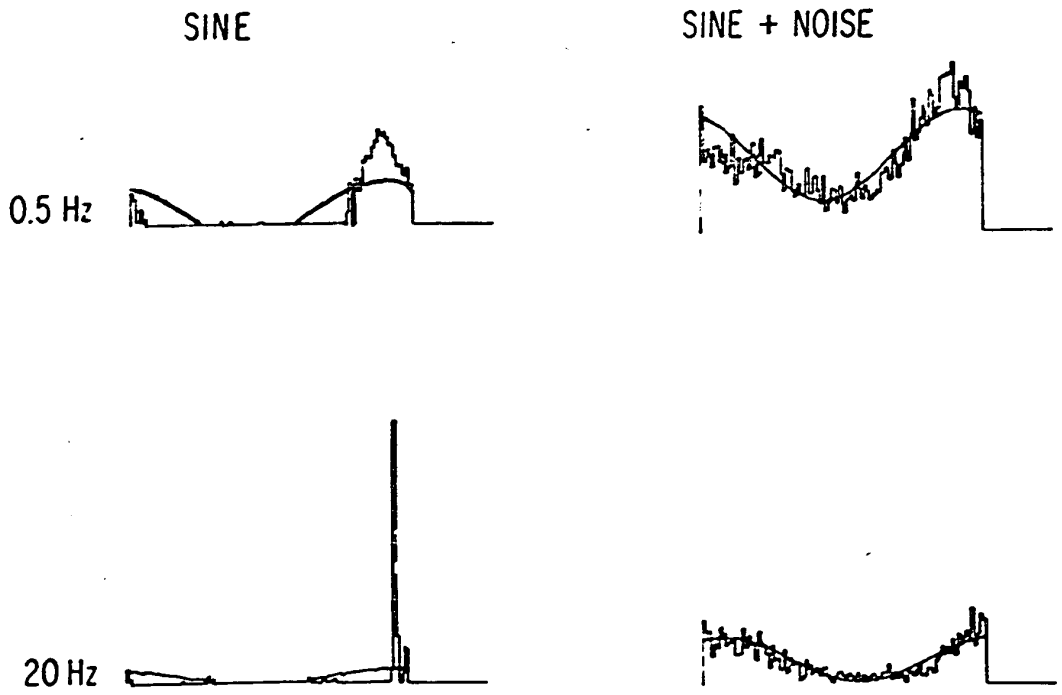

Figure 4.6 . Cycle histograms of the response of a tactile spine to sinusoidal driving functions with and without a stochastic, band-limited auxiliary signal .

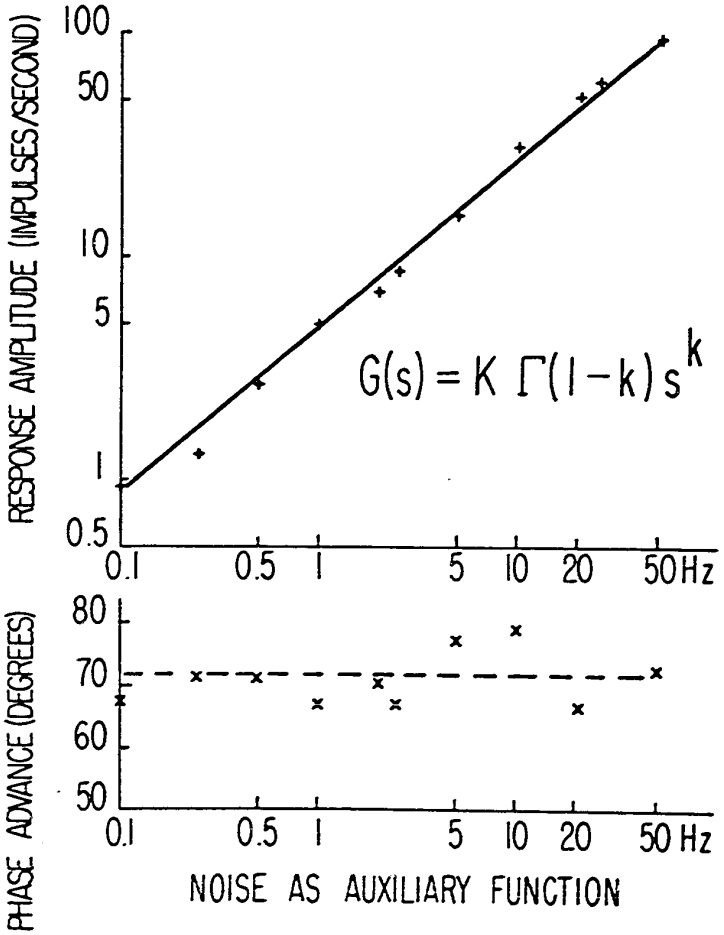

Figure 4. 7 . Bode plot of the frequency response function obtained by using sinusoidal driving functions with a stochastic , band-limited auxiliary signal .

locked pattern to give a response which when averaged is smoothly modulated .

Although use of the auxiliary signal has extended the range over which the linear model of equation 4.2 applies it does not give any measure of how accurately the model fits the system .

Figure 4.8 shows estimates of the spectra of the tension driving function (input spectrum) , the sensory spike train (output spectrum), and the real (co-spectrum) and imaginary (quad-spectrum) parts of the forward cross-spectrum estimated by methods described in chapter 3. They are the average of 50 spectral estimates , each obtained from 2.56 seconds of data sampled at 5msec. intervals . Thus each spectral estimate has approximately 100 degrees of freedom . The input spectrum shows the cut-off characteristics of the filter used to prevent aliasing when the tension record was sampled .

From these spectral estimates use of equations 3.27 , 3.28 and 3.29 provide an estimate of the coherence function and its confidence limits and equations 3.30 , 3.32 and 3.33 provide an estimate of the frequency response function and its confidence limits . These estimates for two receptors are shown in Figure 4.9 .

The extremely low level of the coherence function indicates that the system is nonlinear , and so although the frequency response functions obtained by using different input stimuli (sine waves , rectangular waves , sine waves with auxillary functions and band-limited white noise) are all of the same form the frequency response function is not a good characterization of the input-output relations of the receptor .

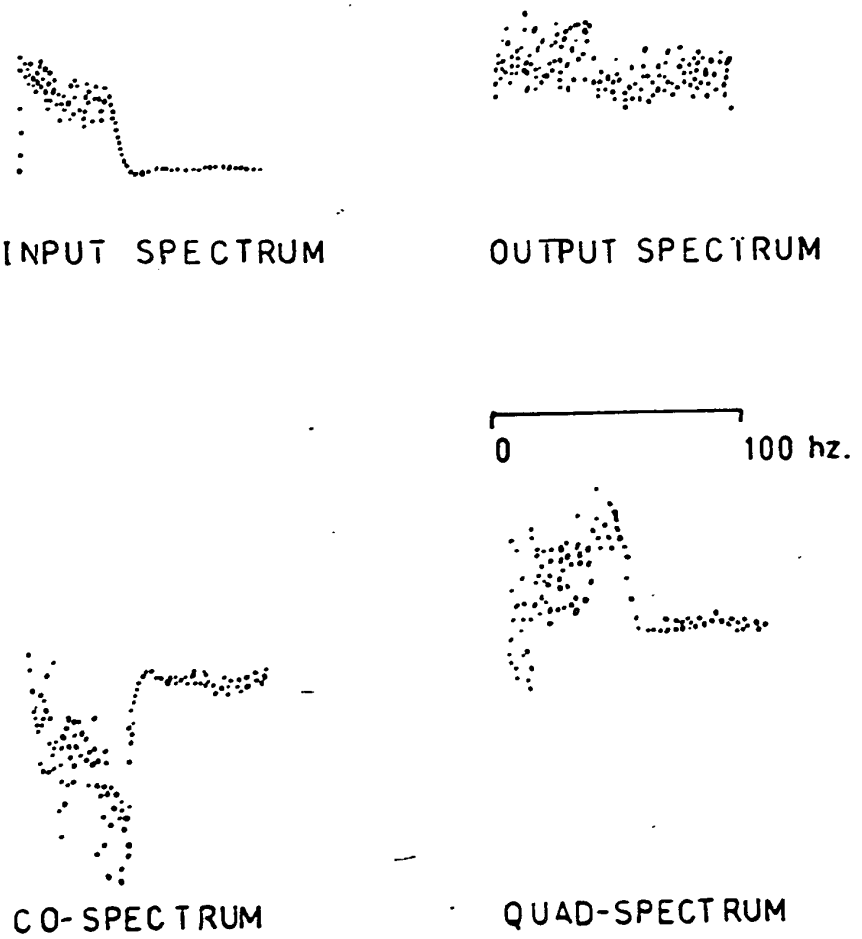

Figure 4. 8 . Estimates of the input , output , and real and imaginary parts of the cross-spectrum when the tactile spine is stimulated by a stochastic , band-limited driving function .

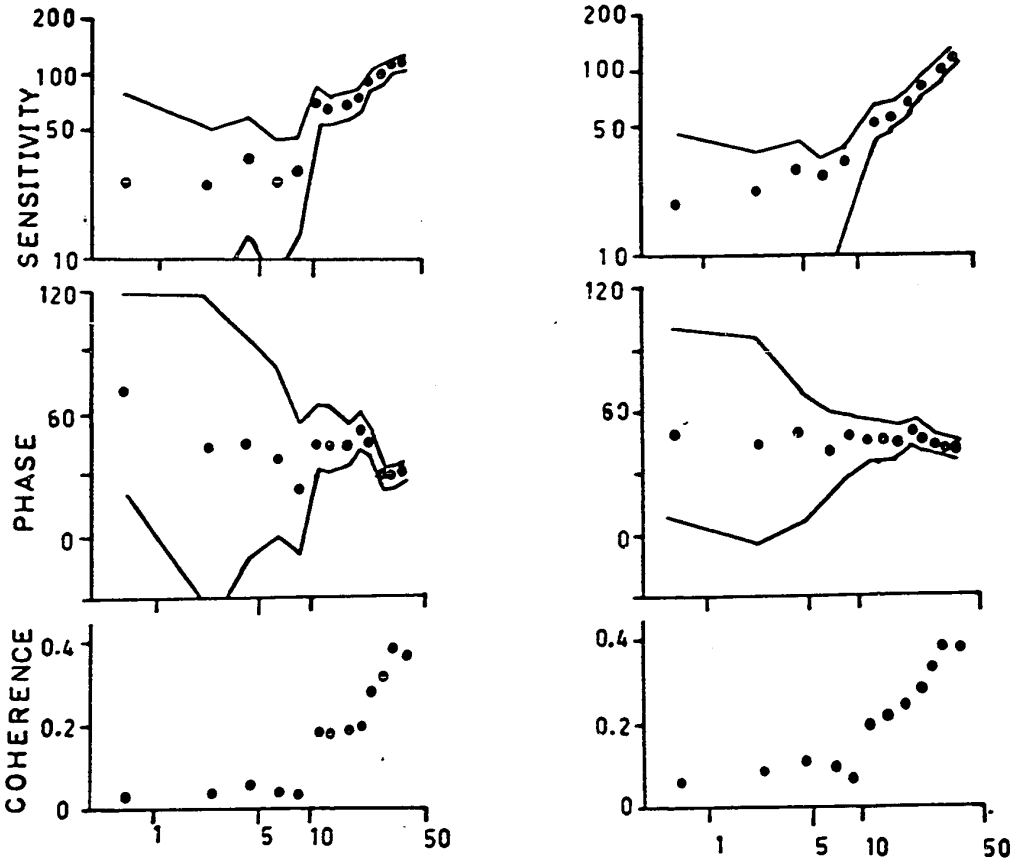

Figure 4. 9 . Bode plots of the frequency response function , and the coherence function , of the tactile spine estimated by using a stocahstic , band-limited driving function .

It has been shown analytically that the coherence function of a perfect or linear voltage to rate convertor can be close to one at frequencies much less than the carrier rate (Stein, French and Holden, 1972) . Similar results have been obtained using a neuronal model of the leaky integrator type (French and Stein, 1970 ; French and Holden, 1971c ; Stein, French and Holden, 1972) . Thus the low value of the coherence function of the spine cannot be entirely due to the threshold properties of the sensory neurone .

95% confidence limits have been drawn around the estimates of the frequency response function . These confidence limits depend on the value of the coherence function (see section 3.10) and since the coherence is low they are very wide . The narrowing of the confidence limits at high frequencies is in part due to the increase in the coherence function at higher frequencies and is also in part due to the plotting algorithm used . Since the frequency axis of a Bode plot is logarithmic , in order to have the plotted points approximately equally separated data points at higher frequencies result from wider frequency segment averaging than points at lower frequencies , and so have a higher number of effective degrees of freedom .

From equation 2.26 the information transmission rate for continuous signals band-limited to 50hz. can be estimated from the coherence function estimates as 6.5 ± 1.2 bits/second for ten preparations .

4.4. Discussion .

The low level of the coherence function means that the frequency response function , however it is estimated , is not a good characterization of the input-output relations of the receptor . Bendat and Piersol (1966) give three possible cases for a coherence function of a system being less than one :

a). the system is nonlinear

b). the system is subject to unobserved inputs which are not correlated with the driving function

c). the system has an intrinsic noise source .

These three cases can occur in any combination .

Since the receptor is silent in the absence of mechanical stimulation of the tactile spine there is no reason to assume that the low coherence of the receptor can be attributed to unobserved inputs . Thus the low coherence can be ascribed to the intrinsic stochastic properties of the receptor and to nonlinearites .

The stochastic properties of the sensory spike train may not be readily quantified as in the absence of a stimulus there is no sensory activity and in the presence of a maintained , constant stimulus the spike train adapts and so is non-stationary .

A possible cause of the low coherence is rectification due to the absence of a carrier rate . Figure 4.10 is a plot of the coherence function of a perfect rectifier estimated by passing band-limited white noise through a Germanium diode . At no frequency is the coherence function greater than 0.75 . Thus rectification alone cannot account for the observed values of the coherence function of

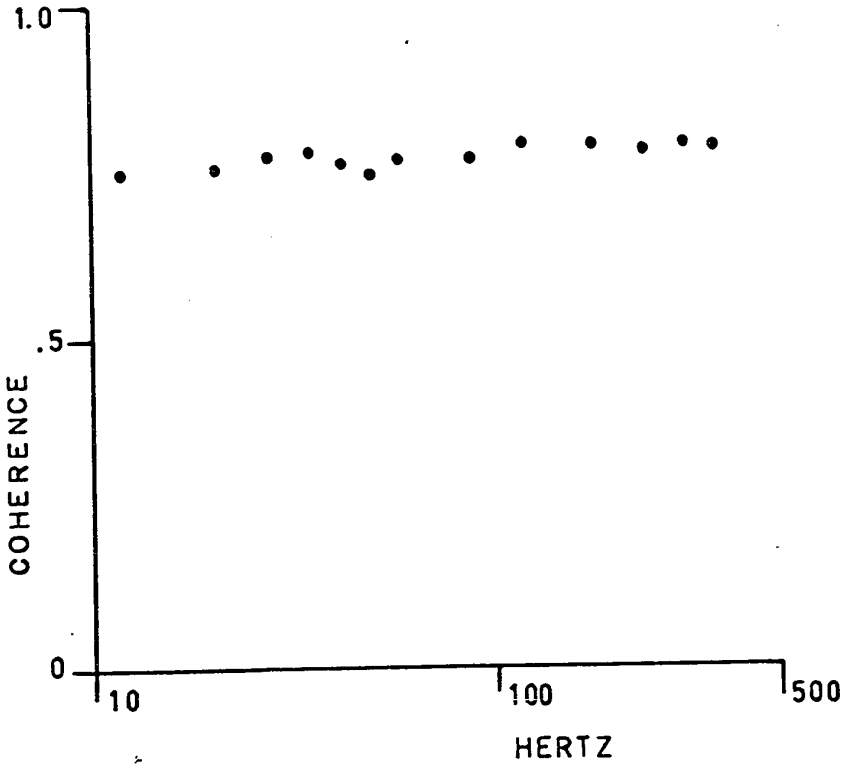

Figure 4.10 . Estimate of the coherence function of a Germanium diode .

the tactile spine .

One unusual aspect of rectification of a pulse train due to the absence of a carrier rate is that the addition of a DC or low frequency signal incoherent with the input driving function can increase the coherence at all frequencies . Figure 4.11 shows the coherence function of a model neurone (French and Stein, 1970) estimated with no bias on the integrator and so a zero carrier rate and with a bias on the integrator producung a carrier rate of 100 impulses/sec. . The coherence function was estimated by subjecting the model neurone to band-limited white noise which in both cases had an input signal root mean squared power of 0.25 volts. The time constant of the leaky integrator was 10 msecs. . The addition of a DC input to the integrator has increased the coherence at all frequencies , and so has increased the information transmission rate estimated by equation 2.26 by 30% . In a linear system the addition of any signal uncorrelated with the input would cause a decrease in the coherence of the system at some frequencies and would not increase the coherence at any frequencies .

Crowe (1967) has pointed out the similarity of the ramp response of the tactile spine to the ramp response of mammalian muscle spindle secondary afferents . The coherence function of the amphibian muscle spindle afferent has been estimated by a different technique (Koles, 1970) and although the values of the coherence function of the spindle are greater than those of the tactile spine the coherence function has the same general shape , that is , increasing at higher frequencies . This contrasts with the coherence function computed

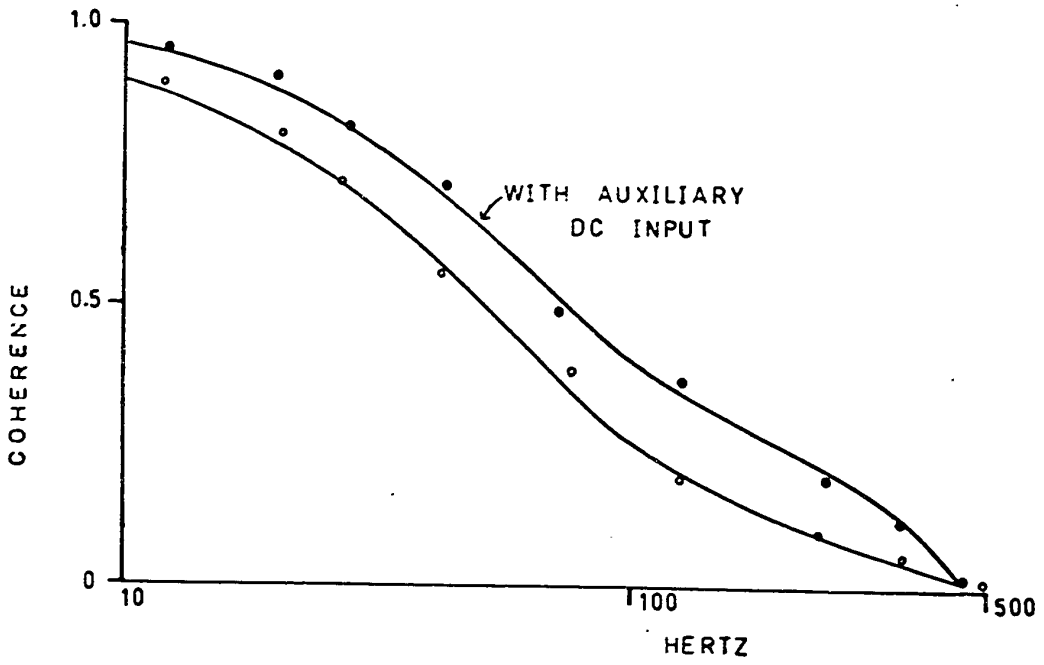

Figure 4. 11 . Estimates of the coherence function of a model neurone with a zero carrier rate and a carrier rate of 100 impulses/second caused by an auxillary DC input .

(Stein, French and Holden,1972) or estimated (French and Holden, 1971c) for simple neuronal models , for which the coherence function decreases with frequency . This increase in the coherence function with frequency may be due to the processes underlying adaptation . The effect of adaptation (produced by increasing the absolute refractory period) on the coherence function of the model neurone is to reduce the coherence at low frequencies while leaving the coherence at high frequencies uneffected . This supports the idea that adaptation gives a receptor a 'high-pass' filter characteristic .

Even though the frequency response function is not a good characterization of the input-output relations of the tactile spine the estimates obtained by using spectral analysis may be fitted by the frequency response function of equation 4.2 . An expression of this form , derived from the power function decay in response to a step input function , has been used to model the input-output relations of a wide range of receptors - the tactile spine of the cockroach (Chapman and Smith, 1963 ; Pearson and Holden, 1970) , the slowly adapting stretch receptor of the crayfish (Brown and Stein, 1966) , carotid body chemoreceptors (Landgren, 1952) and abdominal stretch receptors in butterflies (Weevers, 1966) . Various physical analogs have been proposed which give a power function decay in response to a step input , and a simple abstract model is a series of exponential decay processes which have different time courses .

Chapman and Smith (1963) describe the power function decay as a fractional differentiation of the driving signal . Brown and Stein (1966) point out that the power function provides a means of

encoding information about the driving function and its first derivative . However , because of the low coherence of the receptor , an alternative view would be to consider it as a detector of any sharp or sudden sudden stimulus - although the waveform of the stimulus cannot be reliably recovered from the spike train the fact that a transient had occured could be detected .

CHAPTER 5 .

THE FEMORAL CHORDOTONAL ORGAN OF THE LOCUST .

5.1 . Introduction.

Insect mechanoreceptors and proprioceptors have been divided into five morphological groups : hair plates , campaniform sensilla , stretch receptors , chordotonal organs and statocyst-like organs (Dethier, 1963) . The chordotonal organs are morphologically the most complex kind of mechanoreceptor found in insects . A chordotonal organ consists of a number of sensilla attached to the body wall by a ligament at the axonal end and by accessory cells at the dendritic end . Each sensillum consists of a bipolar sensory neurone and at least two accessory cells . The dendrite of the sensory neurone is enveloped by the two or more accessory cells , and its termination is enclosed by a scolopoid sheath . In spite of extensive electrophysiological and histological investigations of Crustacean chordotonal organs (Wiersma and Boettiger, 1959 ; Whitear, 1962 ; Mendelson, 1963 ; Bush, 1965a , 1965b) the significance of the complex structure of the chordotonal organ is unknown .

Simple , connective chordotonal organs (Howse, 1968) in insects have not been investigated in any great detail . Becht (1958) has described the effects of insecticides on cockroach chordotonal organs , and Hubbard (1959) has published a preliminary study of the femoral chordotonal organ of the locust .

As part of a series of experiments investigating the role of proprioceptive feedback during postural and locomotor activity in locusts Runion and Usherwood (1966) and Usherwood, Runion and Campbell (1968) have described the histology of the femoral chordotonal organ of the locust and have qualitatively investigated its responses and reflex actions .

The femoral chordotonal organ is attached by ligaments to the posterior wall of the femur and by an apodeme to a protrusion on the tibia near the femoro-tibial articulation . It is also attached by ligaments to the apodemes of the extensor and flexor tibiae muscles . Three groups of sensory cells have been described , comprising of a total of 24 bipolar sensory neurones in the chordotonal organ . The sensory axons from the chordotonal organ are contained in metathoracic nerve N_5b_1 [terminology of Campbell, 1961] .

Recordings from the chordotonal organ nerve in response to sinusoidal or ramp changes in the femoro-tibial angle showed that there were both tonic and phasic units . It was not possible to activate single units , but the summed tonic discharge was a linear function of the femoro-tibial angle . The summed tonic discharge adapted to within 90% of a steady level within one minute after a step change in femoro-tibial angle .

Phasic units responded to sinusoidal movements of frequencies from 0.1 to 170 hz. , some units responding to extension and others to flexion . Chordotonal sensory activity during extension of the tibia caused reflex activation of the flexor tibiae muscle , and during flexion caused reflex activation of the slow axon in nerve N_3b to

the extensor tibiae muscle . Generally the response to extension was greater than the response to flexion . With one hz. sinusoidal stimulation the reflex response to the extensor muscle adapted .

5.2 . Methods .

In all experiments adult male locusts (Schistocerca gregaria) , which had been commercially obtained , were used . The metathoracic leg was cut through at the coxa , and the cut surface covered with Vaseline to prevent drying . The leg was mounted on a cork platform so that the tibia was held in the vertical plane . The leg was held rigidly by dental wax , plasticine or glue (Eastman 9-10 adhesive) . The tibia was cut 5 mm. from the femoro-tibial joint and tissue inside the tibial stump macerated by a blunt probe . The femoro-tibial joint was dissected so that the tibia was attached to the femur only by the apodemes of the chordotonal organ and the flexor and extensor tibiae muscles . The tibial stump was held horizontally in a pair of screw forceps attached to the armature of a vibration generator (Pye-Ling model V47) . A small section of the ventral cuticle of the femur two cms. from the femoro-tibial joint was removed and the underlying flexor tibiae muscle dissected away , and N_5 picked up on bipolar silver electrodes . The femoro-tibial joint and the recording electrodes were covered with Vaseline to prevent drying . This minimal dissection avoids exposing the chordotonal organ , as Usherwood, Runion and Campbell (1968) have observed that Vaseline or locust saline (Hoyle, 1953) change the responsiveness of the chordotonal organ .

Movement of the femoro-tibial joint is limited to an angle of 170 degrees , which corresponds to a 1.9 mm. movement of the apodeme of the chordotonal organ . All movements of the tibia were restricted within $\pm$ 0.5 mm. of the extension equivalent to 90 degrees flexion . The vibration generator was driven by the output from a length servo control unit via a power amplifier . The feedback transducer to the servo was a Hewlett-Packard DC input, DC output length transducer (model 24DCDT 050) which had a linear displacement range of $\pm$ 0.050 inches . The command signal to the servo could be a DC level added to

i). the output from a Hewlett-Packard 3300A function generator

ii). the output from a band-limited noise generator .

The closed loop frequency response function of the length servo control system was flat up to 100 hz. .

The amplified action potentials , the output from the length transducer and reference markers were recorded on a Thermionic Products T3000 FM tape recorder for subsequent processing on the LAB-8 computer . Data anlysis was by methods described in chapters 3 and 4 .

5.3 . Results .

An interspike interval histogram of the discharge of a tonic unit from the chordotonal organ is shown in Figure 5.1a . Since an increase in the length of the chordotonal organ , corresponding to an increase in the femoro-tibial angle , causes recruitment of other tonic units records in which a single tonic unit could be reliably extracted by pulse height analysis could only be obtained with low discherge rates . The unit of Figure 5.1a had a mean rate of 10.3

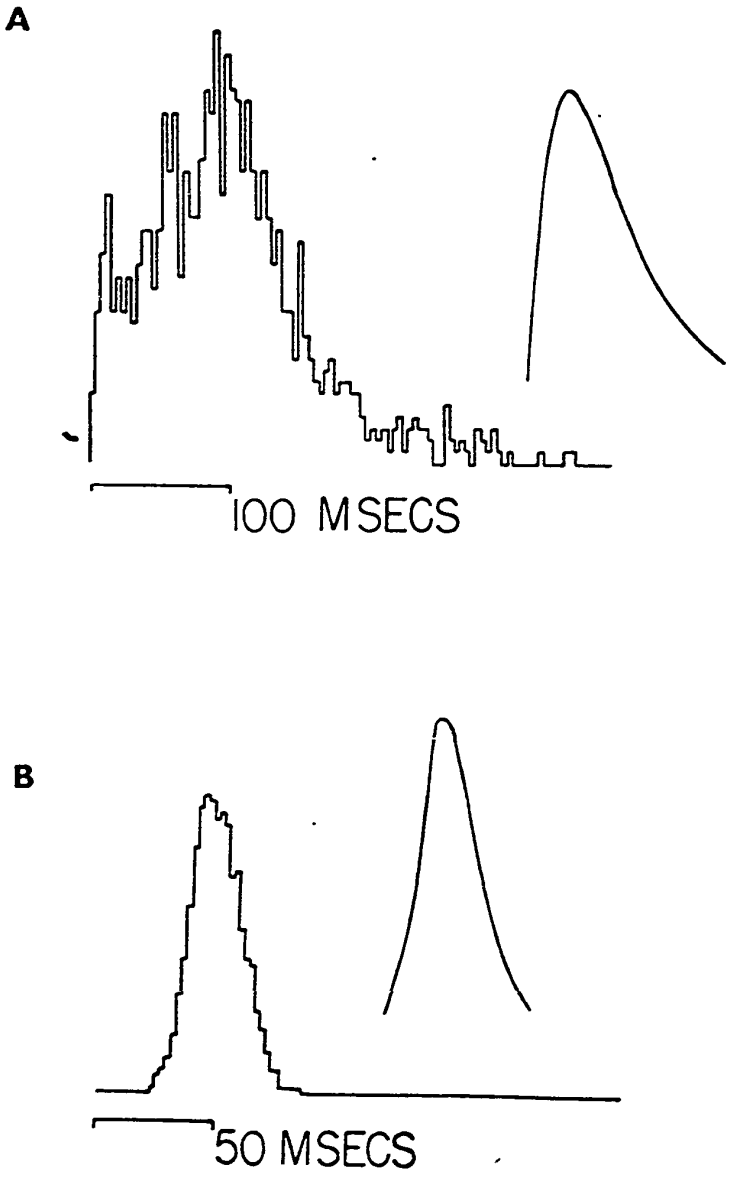

Figure 5.1 . Interspike interval histograms of two tonic units from the femoral chordotonal organ . Inserts show computed Gamma distributions .

impulses/second and a coefficient of variation of the interspike interval of 0.63 . Since the interspike interval histogram is unimodal and positively skewed it seems appropriate to fit it by a Gamma distribution (Cox and Lewis, 1966) . The Gamma distribution is defined by :

$$f(x) = \left[\frac{k}{\mu}\right]^k \frac{x^{k-1} e^{-kx/\mu}}{\Gamma(k)} \qquad 5.1$$

where $\mu = E\{x\}$ and $\Gamma(k)$ is the Gamma function of order k defined by equation 4.3 . The variance of this distribution is μ^2/k and the coefficient of variation is $1/\sqrt{k}$. When k is one the Gamma distribution reduces to the exponential distribution , and when k tends to infinity the Gamma distribution tends to the Normal distribution . Thus the Gamma distribution can encompass a wide range of distributions , however , it does not encompass any negatively skewed , flat , sharply peaked or multimodal distributions .

k , the order of the Gamma distribution may be estimated from :

$$k \sim \frac{1}{\left[\frac{\sigma}{\mu}\right]^2} \qquad 5.2$$

where σ is the standard deviation . Use of equation 5.2 with estimates of the mean and standard deviation of the histogram of Figure 5.1a give the estimate of k as 2.7 . The insert of Figure 5.1a shows the computed Gamma distribution of order 2.7.

This method of estimating k does not produce the least mean square error between k and $\hat{k}$, especially as $\hat{k} < 10$ (Cox and

Lewis, 1966) and so is not an efficient method of estimating k (Bendat and Piersol, 1966) . Cox and Lewis (1966) have shown that a maximum liklihood estimator of k is given by the solution of

$$\log_e(\hat{k}) - \Psi(\hat{k}) = \log_e \bar{\hat{t}} - \frac{\sum_{i=1}^{N} \log_e t_i}{N} \qquad 5.3$$

where

$$\bar{\hat{t}} = \frac{\sum_{i=1}^{N} t_i}{N} \qquad 5.4$$

and $\Psi(\hat{k})$ is the digamma function defined by

$$\Psi(\hat{k}) = \frac{d \log_e \Gamma(\hat{k})}{d\hat{k}} \qquad 5.5$$

Some tonic units fired regularly : Figure 5.1b shows the interspike interval histogram of such a unit , with a mean rate of 20.1 impulses/second and a coefficient of variation of 0.24 . From equation 5.2 this would give an estimate of the order of the distribution k = 17.3 . The computed Gamma distribution of order 17.3 is shown in the insert of Figure 5.1b . The power spectrum estimate of this spike train obtained from 50 non-overlapping samples each of 5.12 seconds is given in Figure 5.2 . This spectrum is typical of a high order Gamma distribution , showing

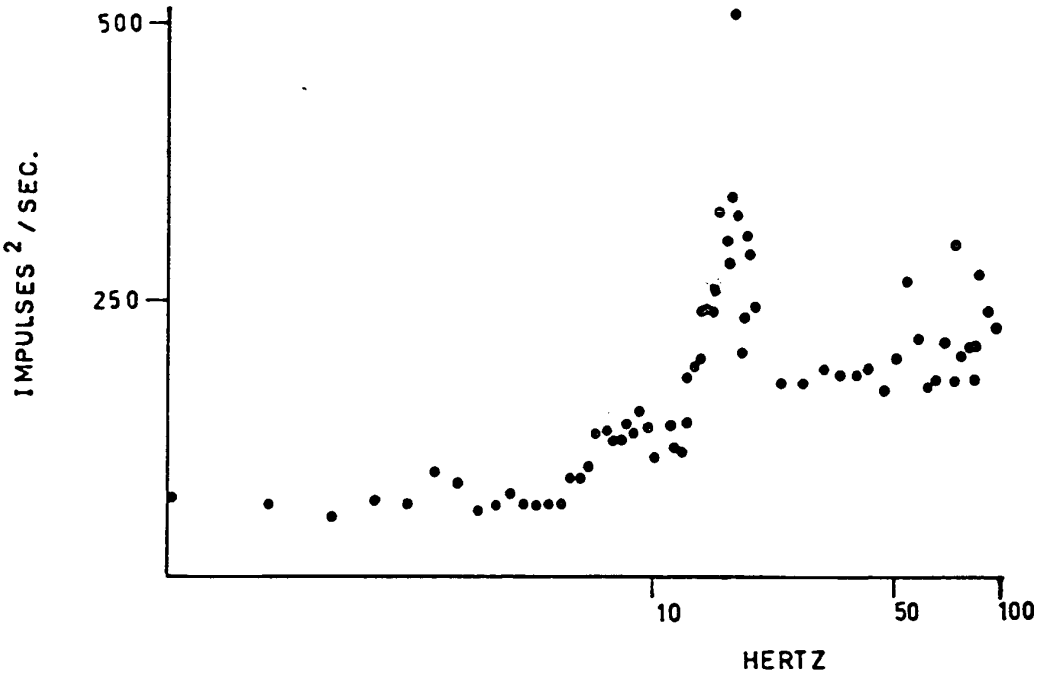

Figure 5.2 . Estimate of the power spectrum of the tonic unit of Figure 5.1b.

the low and high frequency asymptotes and the overshoot at the mean rate .

Cycle histograms of the response of a single unit to sinusoidal driving functions are shown in Figure 5.3 . In contrast to cycle histograms obtained from the tactile spine , the histograms obtained from the chordotonal organ do not show rectification at low driving frequencies . This is because at a constant length the receptor has a variable background discharge or carrier rate which may be smoothly modulated by low frequency sinusoidal driving functions . In the case of the tactile spine of the cockroach rectification was proposed as a partial cause of the low coherence function observed . Thus , if other factors were equal , one might expect that the coherence function of the chordotonal organ would be greater than the coherence function of the tactile spine .

Phase locking in response to sinusoidal driving functions occurs at a frequency higher than that for the tactile spine . At 50 hz. there is one-to-one entrainment .

Figure 5.4 shows estimates of the spectra of the input driving function (input spectrum) , the output spike train of a single unit (output spectrum) , the real part (co-spectrum) and imaginary part (quad-spectrum) of the cross-spectrum when the chordotonal organ was excited by a stochastic , band-limited driving function . These estimates are the average of 50 sample estimates each from 5.12 seconds of data . All the estimates have been normalized to the eleven bit accuracy of SAPA (French and Holden, 1971b) and so no amplitude scale is given . Since there has been no frequency range

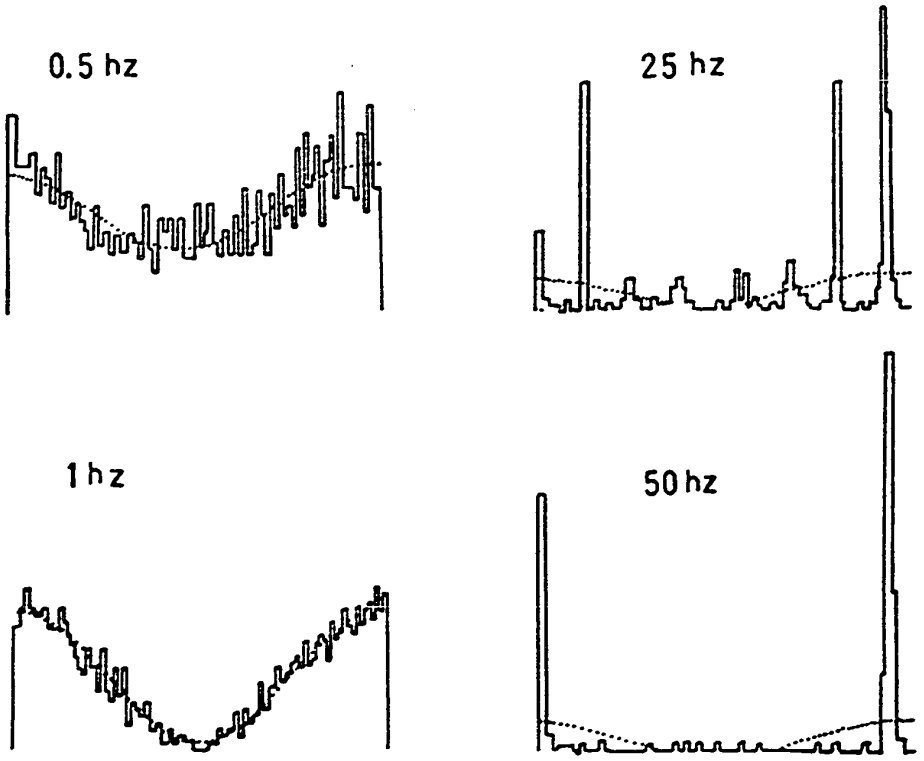

Figure 5.3 . Cycle histograms of the response of a phasic unit from the chordotonal organ to simusoidal driving functions .

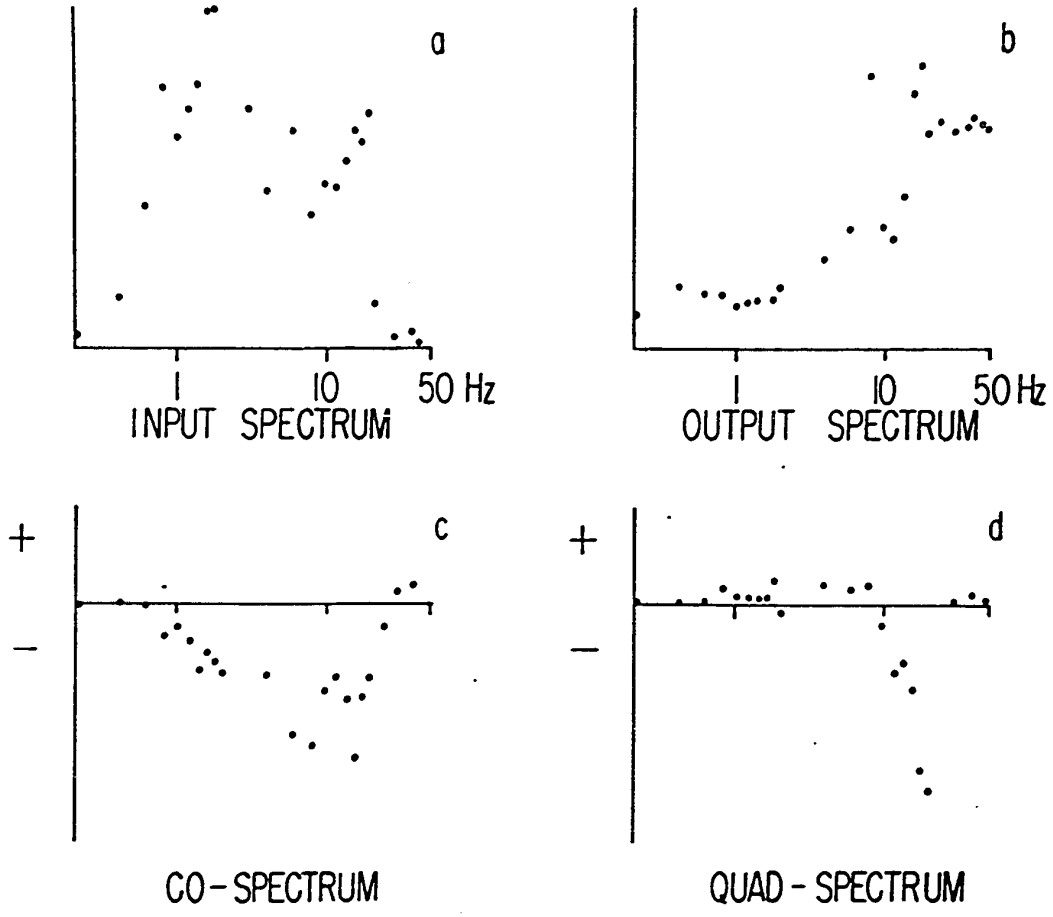

Figure 5.4 . Estimates of the input , output and cross-spectra when the chordotonal organ was excited by a stochastic , band-limited driving function . The ordinates are a logarithmic plot of the SAPB file contents .

averaging the estimates have approximately 100 degrees of freedom .

Estimates of the frequency response function and its confidence limits obtained by using equations 3.30, 3.32 and 3.33 and of the coherence function obtained by using equations 3.27, 3.28 and 3.29 are shown in Figure 5.5 . Because of the low value of the coherence function the 95% confidence limits of the sensitivity curve are wide , but for frequencies less than 10 hz. the sensitivity is approximately constant . Above 10 hz. the sensitivity increases . This simple frequency response curve , illustrated for four different units in Figure 5.6 , is similar to that of a simple high pass filter whose transfer function is given by

$$H(s) = (sT + 1) \qquad 5.6$$

A Bode plot of this transfer function is shown in Figure 5.7 . The corner frequency of the gain curve occurs at 1/T hz. , above which the gain increases at + 6 dB / octave . The slope of the frequency response curves of Figure 5.5 above 10 hz. is about 100 impulses/ second. mm / decade change in frequency . Since below 10 hz. the sensitivity is approximately constant at 10 impulses/sec. mm. if a sensitivity of 10 impulses/sec. mm. is taken as equivalent to a gain of one the slope of the frequency response curve above 10 hz. is equivalent to +20 dB / decade , or +6 dB / octave . This arguement is not strictly valid since the input and output do not have the same dimensions , and so a gain may not be defined ; however ,it does support the simple frequency response function of equation 5.6 .

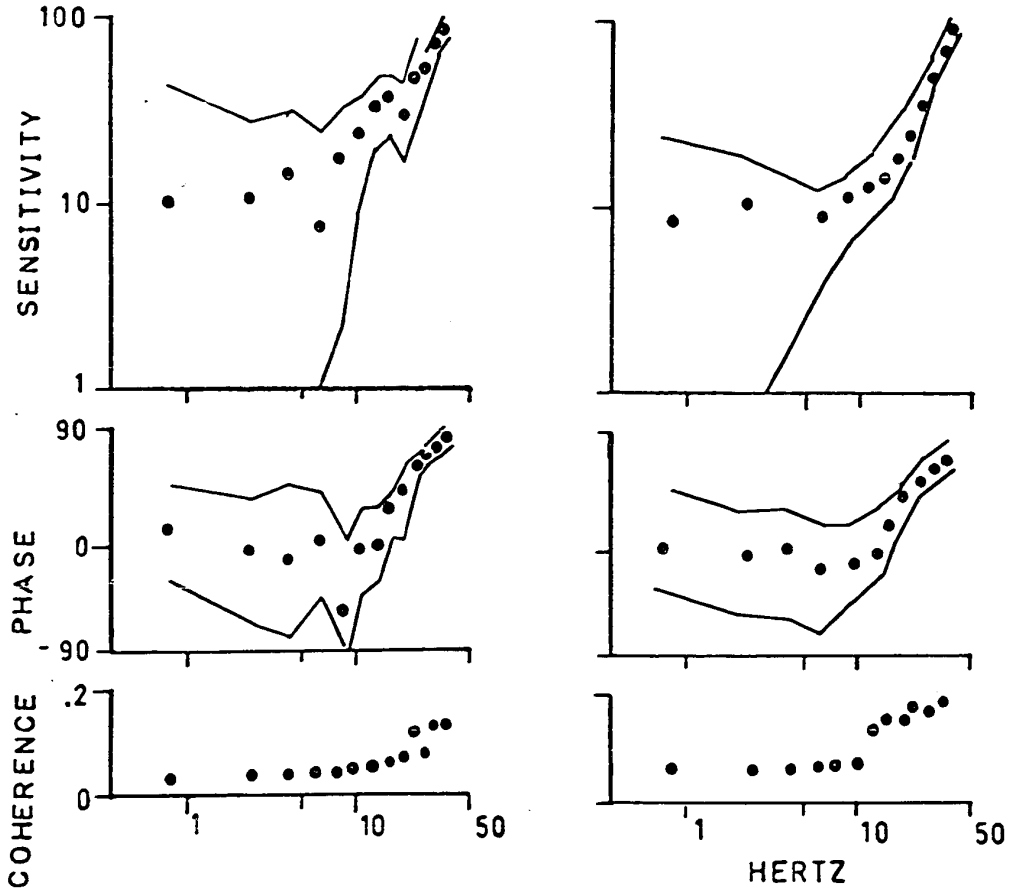

Figure 5.5 . Estimates of the frequency response function of two chordotonal organ units . The sensitivity curves are in impulses/sec. mm. .

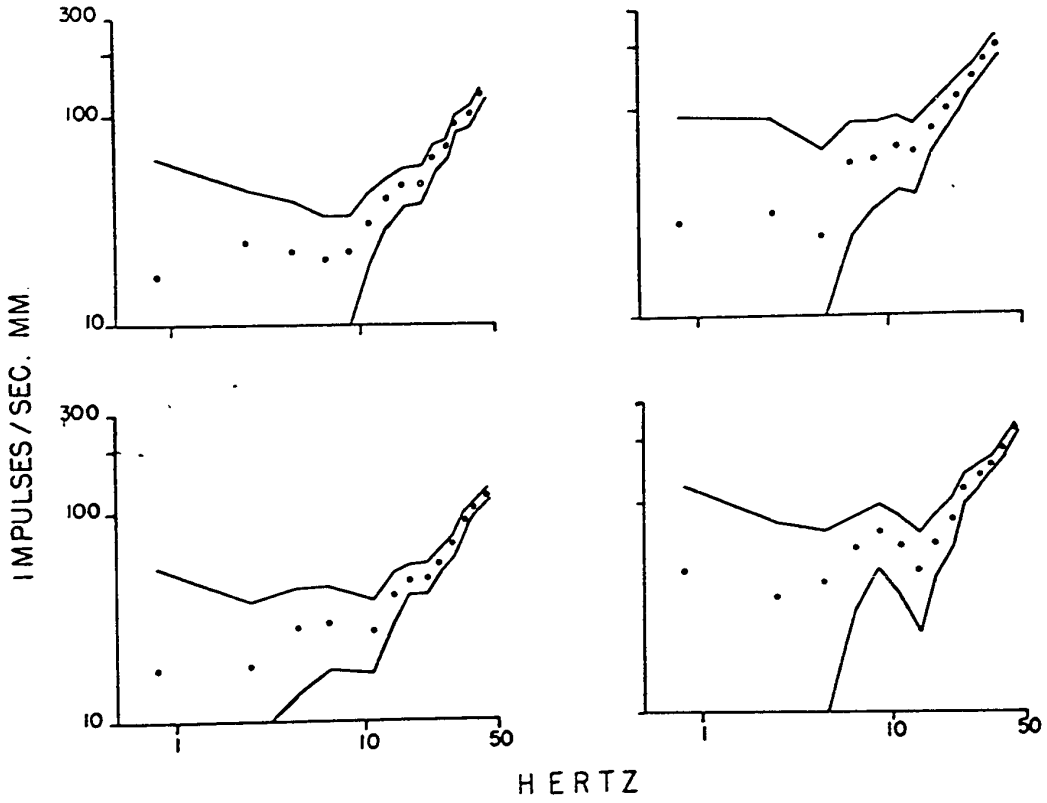

Figure 5.6 . Sensitivity of four chordotonal organ units .

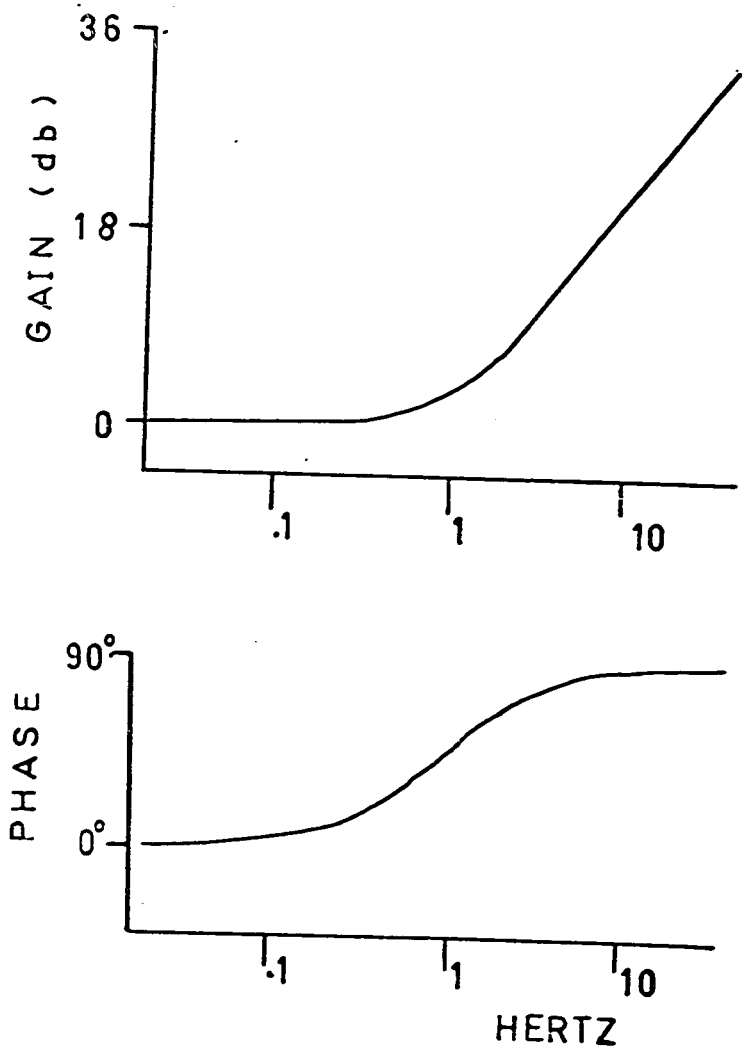

Figure 5.7 . Bode plot of transfer function of equation 5.6 .

Even though the .95% confidence limits are wide the phase advance of the frequency response functions of Figure 5.5 do support the simple frequency response function of equation 5.6 in that the phase advances monotonically from zero to + 90 degrees . However because of the wide confidence limits local maxima suggestive of other terms in the frequency response function would not be detected .

Figure 5.8 shows estimates of the coherence function of four different units . The coherence function is less than 0.5 at all frequencies , and extremely low at frequencies less than 10 hz. These coherence function curves have a similar shape to those for the cockroach tactile spine (Chapter 4) and the amphibian muscle spindle (Koles, 1970) . The value of the coherence function is higher than that for the cockroach tactile spine , as was predicted from the absence of rectification in the cycle histograms in response to sinusoidal driving functions .

The arrows on the coherence function curves of Figure 5.8 mark the mean firing rate of the unit . In experiments using an electronic neural analog (French and Stein, 1970) the coherence function drops sharply before the mean firing rate or carrier rate and is low above the carrier rate (French and Holden, 1971c ; Stein, French and Holden, 1972) . This is not observed in the coherence function estimates for the chordotonal organ . This can be explained as in the case of the neural anlog the driving function modulated the carrier rate , which was the mean firing rate . However , in the case of the chordotonal organ , the resting rate is variable , and the mean rate is caused by the phasic response to the driving function , and so is

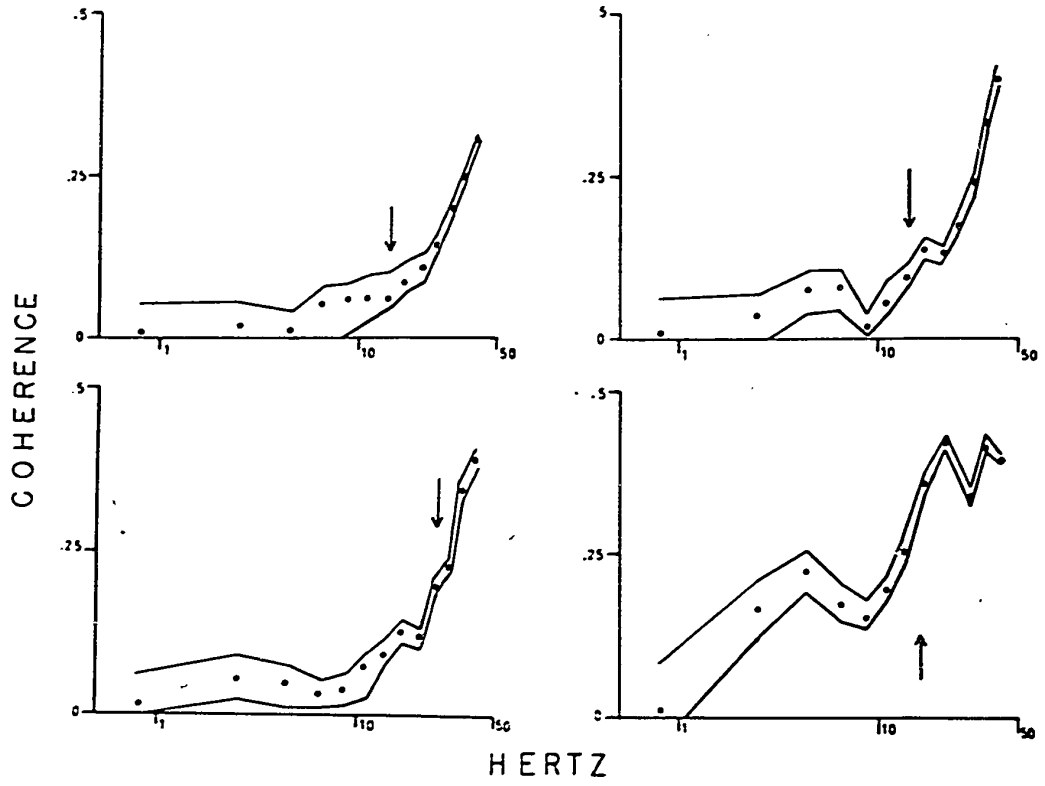

Figure 5.8 . Coherence function of four chordotonal organ units .

not entirely analogous to a carrier rate .

The coherence function of the electronic neural analog is a function of the input RMS power (French and Holden, 1971c ; Stein, French and Holden, 1972) . Figure 5.9 shows coherence function estimates for a single chordotonal organ unit at three different RMS power values of input length driving function . The estimates have more than a hundred degrees of freedom . The coherence increases with the input amplitude , especially at high frequencies . This contrasts with the results from the electronic neural analog , in which the increase in coherence with input amplitude was predominantly at frequencies less than the carrier rate . This increase in coherence at high frequencies supports the idea that the receptor acts as a high pass filter .

The information transmission rate of chordotonal organ single units calculated by equation 2.26 ranged from 8.75 to 27.7 bits/second . Since the coherence function increases with input amplitude the information transmission rate increases with the amplitude of the driving function .

5.4 . Discussion .

The frequency response functions obtained by spectral analysis indicate that although the coherence function is low , and so a linear model is not an accurate characterization of the input-output relations of the receptor , the best-fitting linear model is very similar to a simple lead filter whose transfer function is given by equation 5.6 and shown in Figure 5.7 . A possible cause for this extremely simple transfer function might be the visco-elastic properties of the

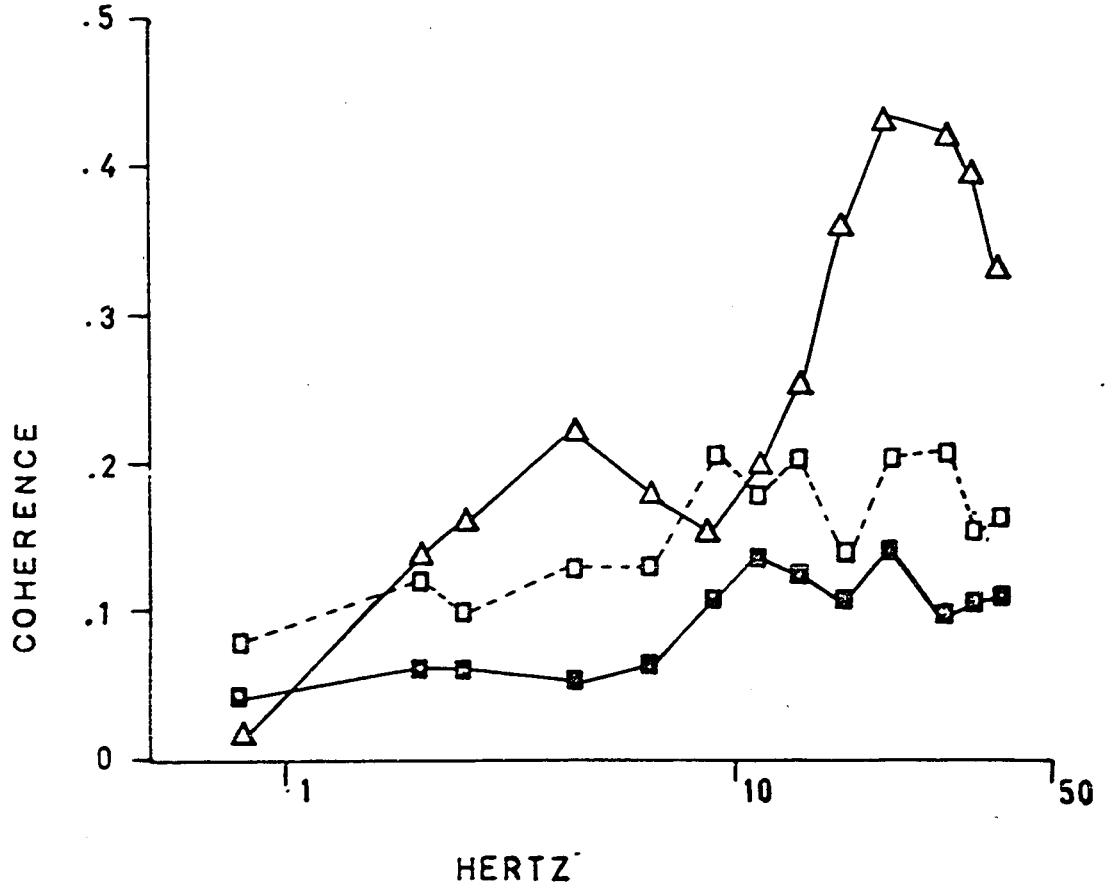

Figure 5.9 . Estimates of the coherence function of a chordotonal organ unit at three different input amplitudes .

apodeme of the chordotonal organ .

The low coherence of chordotonal organ single units at frequencies below 10 hz. means that the waveform of slow changes of the femoro-tibial angle may not be accurately recovered from the spike train of a single unit by any linear operation . Changes in the femoro-tibial angle at frequencies from 10 hz. to 50 hz. may only be partially recovered by a linear operation on a single spike train . The dependence of the coherence function on the amplitude of the driving function means that more information may be recovered by a linear operation on the spike train about large amplitude movements than about small amplitude movements .

Usherwood,Runion and Campbell (1968) have reported that destruction of the femoral chordotonal organs produce significant changes in postural and locomotor behaviour . This has been used to support the concept that proprioceptive feedback is very important in the generation of normal postural and walking behaviour . This concept implies that the proprioceptors can provide the central nervous system with detailed information about position and movement , and that this information can be 'decoded' or utilized by the central nervous system in the normal control of movement . During walking and postural activity movements of the femoro-tibial angle are slow , and occur at frequencies where the coherence of single chordotonal organ units is very low . This low coherence means that detailed proprioceptive information cannot be recovered from the spike train of a chordotonal organ single unit by any linear operation . Mountcastle (1967) has reviewed

evidence that supports the hypothesis that the processing of sensory information by the nervous system is by approximately linear operations . If the 'decoding' operations performed on the spike train of a single chordotonal organ unit are approximately linear then the single unit cannot provide the central nervous system with detailed proprioceptive information . This could be used to argue against the importance of proprioceptive feedback from the chordotonal organ during the normal control of postural and locomotor activity .

However , each femoral chordotonal organ contains about 24 bipolar sensory neurones . If the central nervous system averaged the response of all those chordotonal organ units which had the same properties then the chordotonal organ might provide the central nervous system with detailed proprioceptive information which could be recovered by a linear operation .

This would be supported if the coherence between the length of the chordotonal organ and the reflex motor discharge was greater than the coherence between the length of the chordotonal organ and a single unit . However , preliminary experiments with headless locusts give a very low coherence between length of the chordotonal organ and the reflex discharge in the slow axon of N_3b to the extensor tibiae muscle . This low coherence may be due to other inputs to the motor neurone which might be removed by isolating the ganglion from all inputs apart from N_5 .

CHAPTER 6 .

DISCUSSION .

All physical systems are nonlinear , and so if linear systems theory is to be used to formulate an abstract model to describe the input-output relations of a physical system some measure of the accuracy of the model is essential . When the physical system is a sensory neurone which responds to a continuous driving function by a train of action potentials there is considerable non-harmonic distortion , and so harmonic distortion, however measured , is not a good measure of the linearity of the system . The coherence function , defined by equation 2.22 , provides a measure of the linearity of the relation between the input and output which is sensitive to all kinds of nonlinearities and to intrinsic noise . The coherence function can only be estimated by subjecting the system to a broad band driving function , and using consistent , alias and bias free spectral analysis . If that part of the output which is linearly related to the input driving function is considered to be the signal , and that part of the output which is not linearly related to the input is considered to be noise , then the coherence function is related to the signal-to-noise ratio as shown in equation 2.24 . If the input driving function is a sinusoid , which has a line spectrum , then the signal-to-noise ratio will be infinite and so the coherence function will be equal to one . Thus inputs which have line or very narrow band spectra , which are simple deterministic functions of time , cannot be used to

estimate the coherence function .

There are a variety of methods which may be used to estimate the spectral density matrix of section 2.3 . The rediscovery of the Fast Fourier Transform algorithm (Cooley and Tukey, 1965) has made the direct method of spectral estimation computationally economical , and the development of alias-free sampling of stochastic point processes with a regular sampling interval (French and Holden, 1971a , 1972) has permitted the use of the Fast Fourier Transform algorithm in the estimation of the spectrum of a spike train [when the spike train is treated as a realization of a stochastic point process or as a series of unit impulses] and of the cross-spectrum between two spike trains or between a spike train and a continuous signal .

The direct method of spectral estimation has been implemented on a small computer , and the consistency of the estimates has been achieved by averaging spectral estimates from non-overlapping samples . A better method of consistent spectral estimation would be to average spectral estimates from samples with a 50% overlap (Welch, 1967) . However , implementation of this technique on a small computer would necessitate a large , bulk storage device such as a magnetic tape unit in order to store the entire record and then sequentially access overlapping segments . If such a storage device were available it would permit the computation of spectral estimates with the number of data points greater than the number of core memory locations (Brenner, 1969) .

Consistent spectral estimates provide a means of estimating the frequency response function as well as the coherence function , and

from the coherence function and the number of degrees of freedom of the spectral estimates the confidence limits of the frequency response function can be computed . In both the tactile spine of the cockroach and the chordotonal organ of the locust the sensitivity of the frequency response function increased at higher frequencies , as did the coherence . Thus the estimate of the frequency response function was less stable at low frequencies than at high frequencies . If the input driving function had been shaped so that there was more power present at low frequencies than at high frequencies the stability of the frequency response function would have been more even .

From the coherence function estimate the information transmission rate of the receptor could be estimated by use of equation 2.26 . This is not an estimate of the information capacity of the receptor as the information capacity is defined as the maximum possible transmission rate . This would only be achieved if the input driving function had a spectrum so that most of the input power was at frequecies where the coherence was highest . Previous estimates of the information transmission rate of receptors have been limited to quantifying the ability of the receptor to transmit information about a steady level (Werner and Mountcastle, 1965 ; Darian-Smith et al, 1968 ; Stein, 1968b ; Matthews and Stein, 1969b) . Thus the estimates obtained by use of equation 2.26 for the tactile spine and the chordotonal organ are higher than those reported for other receptors .

Since the nervous system is made up of a large number of neurones it might be argued that the detailed analysis of the input-output relations of a single receptor does not help very much in understanding

the functioning of the nervous system . The spectral density matrix of section 2.3 may be generalized for a system with an arbitrary number of inputs and outputs . Thus the methods described in Chapters 2 and 3 and applied in Chapters 4 and 5 can be generalized to systems with several inputs and several outputs . The complexity of the system to be analyzed by these methods is only restricted by the number of units which may be recorded and the size of the data processing system . Thus when it is possible to record from a large number of neurones simultaneously the methods of Chapters 2 and 3 could provide a means of dealing with the large amount of data .

The driving function to the receptors studied was a function of time only . However , many sensory systems respond to driving functions which are functions of spatial variables as well as of time . Spectral analysis is readily generalized to include n-dimensional functions and so the methods developed in this thesis can provide the background to an approach to more complex aspects of sensory information transmission .

REFERENCES

Akaike, H. 1962. On the design of lag window for the estimation of spectra. Ann. Inst. Stat. Math. (Tokei Suri Kenkyojo Tokyo Annals) 14:1.

Akaike, H. 1964. Statistical measurement of frequency response function. Ann. Inst. Stat. Math. (Tokei Suri Kenkyojo Tokyo Annals) Suppl. 3:5.

Akaike, H. 1969. Power spectrum estimation through autoregressive model fitting. Ann. Inst. Stat. Math. (Tokei Suri Kenkyojo Tokyo Annals) 21:407.

Akaike, H. 1970. On a semi-automatic power spectrum estimation procedure. Proc. 3rd Hawaii Conf. System Sci. 974.

Akaike, H. and Y. Yamanouchi. 1962. On the statistical estimation of frequency response function. Ann. Inst. Stat. Math. (Tokei Suri Kenkyojo Tokyo Annals) 14:23.

Amos, D.E. and L.H. Koopmans. 1963. Tables of the distribution of the coefficient of coherence for stationary bivariate Gaussian processes. Sandia Corp. Monograph SCR-483.

Arden, G.B. 1969. The excitation of photoreceptors. Prog. Biophys. Mol. Biol. 19:373.

Barbi, M. and D. Patracchi. 1971. Spike amplitude modulation at high stimulation frequencies. Kybernetik 8:45.

Bartlett, M.S. 1963. The spectral analysis of point processes. J. Roy. Stat. Soc. B25:264.

Bayly, E.J. 1968. Spectral analysis of pulse frequency modulation in the nervous system. I.E.E.E. Trans. Bio-Med. Engng. BME-15:257.

Becht, G. 1958. Influence of DDT and lindane on chordotonal organs in the cockroach. Nature 181:777.

Bendat, J.S. 1962. Interpretation and application of statistical analysis for random physical phenomena. Trans. I.R.E. BME-9:31.

Bendat, J.S. and A.G. Piersol. 1966. Measurement and analysis of random data. John Wiley:New York.

Benignus, V.A. 1969a. Computation of coherence and regression spectra using the FFT. COMMON, Proc. Houston Meeting, Dec. 9-11, 1968.

Benignus, V.A. 1969b. Estimation of the coherence spectrum and its confidence interval using the Fast Fourier Transform. I.E.E.E. Trans. Audio. Electro-Acous. AU-17:145.

Beutler, F.J. 1970. Alias-free randomly timed sampling of stochastic processes. I.E.E.E. Trans. Inform. Theory IT-16:147.

Bingham, C., M.D. Godfrey and J.W. Tukey. 1967. Modern techniques of power spectrum estimation. I.E.E.E. Trans. Audio. Electro-Acous. AU-15:56.

Blackman, R.B. and J.W. Tukey. 1958. The measurement of power spectra from the point of view of communications engineering. Dover:New York.

Booton, R.C. Jr. 1952. Non-linear control systems with statistical inputs. M.I.T. Dynamic Analysis and Control Laboratory, Report #61.

Borsellino, A., R.E. Poppele and C.A. Terzuolo. 1965. Transfer functions of the slowly adapting stretch receptor organ of crustacea. Symp. Quant. Biol. 30:581.

Brenner, N.M. 1969. Fast Fourier Transform of externally stored data. I.E.E.E. Trans. Audio. Electro-Acous. AU-17:128.

Brown, M.C. and R.B. Stein. 1966. Quantitative studies on the slowly adapting stretch receptor of the crayfish. Kybernetik 3:175.

Brumbach, R.P. 1968. Digital computer routines for power spectral analysis. General Motors Corp., A.C. Electronics - Defense Research Laboratory, Sea Operations Department, Santa Barbara, California. TR68-31 Nonr. 428(00).

Bush, B.M.H. 1965a. Proprioception by the coxo-basal chordotonal organ, CB, in the legs of the crab, Carcinus maenas. J. Exp. Biol. 42:285.

Bush, B.M.H. 1965b. Proprioception by chordotonal organs in the mero-carpopodite and carpo-propodite joints of Carcinus maenas. Comp. Biochem. Physiol. 14:185.

Bush, B.M.H. and A. Roberts. 1968. Resistance reflexes from a crab muscle receptor without impulses. Nature 218:1171.

Campbell, J.I. 1961. The anatomy of the nervous system of the mesothorax of Locusta migratoria migratoriodes (R. & F.). Proc. Zoo. Soc. Lond. 137:403.

Chapman, K.M. and T.R. Nichols. 1969. Electrophysiological evidence that cockroach tibial tactile spines have separate sensory axons. J. Insect Physiol. 15:2103.

Chapman, K.M. and R.S. Smith. 1963. A linear transfer function underlying impulse frequency modulation in a cockroach mechanoreceptor. Nature 197:699.

Cooley, J.W., P.A.W. Lewis and P.D. Welch. 1967. The Fast Fourier Transform and its applications. I.B.M. Watson Res. Center, New York. RC 1743.

Cooley, J.W., P.A.W. Lewis and P.D. Welch. 1969. The finite Fourier Transform. I.E.E.E. Trans. Audio. Electro-Acous. AU-17:77.

Cooley, J.W. and J.W. Tukey. 1965. An algorithm for the machine calculation of complex Fourier series. Math. Comput. 19:297.

Cox, D.R. and P.A.W. Lewis. 1966. The statistical analysis of series of events. Methuen:London.

Crowe, A. 1967. Studies on the transfer function of a cockroach mechanoreceptor. Comp. Biochem. Physiol. 20:13.

Danielson, G.C. and C. Lanczos. 1942. Some improvements in practical Fourier analysis and their application to X-ray scattering from liquids. J. Franklin Inst. 233:365.

Darian-Smith, I., M.J. Rowe and B.J. Sessle. 1968. "Tactile" stimulus intensity: Information transmission by relay neurones in different trigeminal nuclei. Science 160:791.

D'Azzo, J.J. and C.H. Houpis. 1966. Feedback control system analysis and synthesis. McGraw-Hill:New York.

Dethier, V.G. 1963. The physiology in insect senses. Methuen:London.

Dodge, F.A., B.W. Knight and J. Toyoda. 1968. How the horseshoe crab eye processes optical data. I.B.M. Watson Research Laboratory, New York. RC 2248 (#11117).

Enochson, L.D. and N.R. Goodman. 1965. Gaussian approximations to the distribution of sample coherence. Air Force Flight Dynamics Laboratory, Wright-Patterson Air Force Base. Technical Report AFFDL-TR-65-57.

Foster, M.R. and N.J. Guinzy. 1967. The coefficient of coherence: Its estimation and use in geophysical data processing. Geophys. 32:602.

French, A.S. 1970. PULSE, an event/time histogramming program for the Digital Equipment Corporation LAB-8 computer and FNEW-PULSE, a function generating routine for use with PULSE and FOCAL. Comput. Prog. Bio-Med. 1:105.

French, A.S. 1971. SAP9: A program for the rapid computation of consistent spectral estimates. Unpublished.

French, A.S. and A.V. Holden. 1971a. Alias-free sampling of neuronal spike trains. Kybernetik. In press.

French, A.S. and A.V. Holden. 1971b. Frequency domain analysis of neurophysiological data. Comput. Prog. Bio-Med. 1:219.

French, A.S. and A.V. Holden. 1971c. Spectral analysis of information transfer through single units. Presented at 4th Ann. Winter Conf. Brain Res., Aspen, Colorado.

French, A.S. and A.V. Holden. 1972. Semi-on-line implementation of an alias-free sampling system for neuronal signals. Submitted to Comput. Prog. Bio-Med.

French, A.S., A.V. Holden and R.B. Stein. 1972. The estimation of the frequency response function of an insect mechanoreceptor. Submitted to J. Gen. Physiol.

French, A.S. and R.B. Stein. 1970. A flexible neural analog using integrated circuits. I.E.E.E. Trans. Bio-Med. Engng. BME-17:248.

Gentleman, W.M. and G. Sande. 1966. Fast Fourier Transforms - for fun and profit. A.F.I.P.S. Fall Joint Comput. Conf. 26:563.

Gersch, W. 1970. Spectral analysis of EEG's by autoregressive decomposition of time series. Math. Biosci. 7:205.

Gestri, G., L. Maffei and D. Petracchi. 1967. Amplitude modulation of retinal ganglion cell impulses. Kybernetik 4:37.

Gold, R. and C.M. Rader. 1969. Digital processing of signals. McGraw-Hill: New York.

Good, I.J. 1965. The estimation of probabilities: An essay on modern Bayesian methods. M.I.T.:Cambridge.

Goodman, N.R. 1957. On the joint estimation of the spectra, cospectrum and quadrature spectrum of a two-dimensional stationary Gaussian process. Engineering Statistics Laboratory, New York Univ. Scientific paper #10.

Hagiwara, S. and H. Morita. 1962. Electrotonic transmission between two nerve cells in leech ganglion. J. Neurophysiol. 25:721.

Hinich, M.J. and C.S. Clay. 1968. The application of the discrete Fourier Transform in the estimation of power spectra, coherence and bispectra of geophysical data. Rev. Geophys. 6:347.

Holden, A.V. and A.S. French. 1971a. Spectral analysis of receptor dynamics. Can. Physiol. 2:14.

Holden, A.V. and A.S. French, 1971b. Spectral analysis of neuronal interactions. Abstracts, 25th Int. Cong. Physiol. Sci., Munich, 1971.

Houk, J. and W. Simon. 1967. Responses of golgi tendon organs to forces applied to muscle tendon. J. Neurophysiol. 30:466.

Howse, P.E. 1968. Structure and organization of chordotonal organs. Symp. Zoo. Soc. Lond. 23:167.

Hoyle, G. 1953. Potassium ions and insect nerve muscle. J. Exp. Biol. 30:121.

Hubbard, S.J. 1959. Femoral mechanoreceptors in the locust. J. Physiol. 147:8P.

Jenkins, G.M. 1963. An example of the estimation of a linear open loop transfer function. Technometrics 5:227.

Jenkins, G.M. and D.G. Watts. 1968. Spectral analysis and its applications. Holden-Day:San Francisco.

Jones, R.H. 1965. A reappraisal of the periodogram in spectral analysis. Technometrics 7:531.

Kaplan, W. 1962. Operational methods for linear systems. Addison-Wesley: Reading, Massachusetts.